Different immunomodulatory role of Ly6G^{hi} and Ly6G^{int} neutrophils during antiviral antibody therapy

Authors:

Jennifer Lambour[1], Mar Naranjo-Gomez[1,2], Myriam Boyer-Clavel[3] and Mireia Pelegrin[1,2] *

Address:

[1] IGMM, Univ Montpellier, CNRS, Montpellier, France
[2] Current address: IRMB, Univ Montpellier, INSERM, CNRS, Montpellier, France
[3] Montpellier Ressources Imagerie, Biocampus, Univ Montpellier, CNRS, Montpellier, France

***Corresponding author and Lead contact:**

Mireia Pelegrin

Institute of Molecular Genetics of Montpellier

1919, route de Mende

34293 Montpellier Cedex 5

France

mireia.pelegrin@inserm.fr

Keywords : antiviral immune responses, monoclonal antibodies, immunotherapy, immunomodulation, vaccinal effects, immune complexes, neutrophils heterogeneity, monocytes, FcγR.

SUMMARY

Antiviral monoclonal antibodies (mAbs) can generate protective immunity through immune complexes (IC)-FcγRs interactions. We have shown the essential role of neutrophils in mAb-induced immunity of retrovirus-infected mice. Using this model, here we addressed how viral infection, with or without mAb therapy, affects neutrophils' functional activation. We found that neutrophils activated by viral ICs secreted high levels of chemokines able to recruit monocytes and neutrophils themselves. Moreover, inflammatory cytokines potentiated chemokines and cytokines release by IC-activated cells and induced FcγRs upregulation. Similarly, infection and mAb-treatment upregulated FcγRs expression on neutrophils and enhanced their cytokines and chemokines secretion. FcγRs upregulation allowed to identify *in vivo* two splenic neutrophils subpopulations with distinct phenotypic and functional properties that differentially and sequentially collaborate with inflammatory monocytes to induce Th1-type responses in mAb-treated mice. Our work provides novel findings on the heterogeneity and the immunomodulatory role of neutrophils in the enhancement of immune responses upon antiviral mAb therapy.

63 **INTRODUCTION**
64

65 The development of powerful antiviral monoclonal antibodies (mAbs) has provided new therapeutic
66 opportunities to treat severe viral infections (Dibo et al., 2019; Hooft van Huijsduijnen et al., 2020;
67 Salazar et al., 2017; Wang and Zhang, 2020). Fc-dependent mechanisms are crucial for efficient
68 antiviral activity of neutralizing mAbs through the engagement of IgG receptors (FcγRs) expressed on
69 immune cells. These Fc-FcγR interactions lead to the elimination of viral particles and virus-infected
70 cells through phagocytic and cytotoxic mechanisms (i.e. antibody-dependent cellular phagocytosis
71 (ADCP), antibody-dependent cell-mediated cytotoxicity (ADCC),…) (Bournazos and Ravetch, 2017a;
72 Lu et al., 2018). Moreover, studies in different animal models of viral infection, including ours, have
73 provided evidence that mAbs can also enhance antiviral immune responses (so called "vaccinal
74 effects") in a Fc-dependent manner (Pelegrin et al., 2015). These vaccinal effects have been recently
75 reported in HIV-infected patients treated with broadly neutralizing mAb (bnAbs) (Naranjo-Gomez and
76 Pelegrin, 2019; Niessl et al., 2020; Schoofs et al., 2016) although the mechanisms involved have not
77 been identified thus far. The elucidation of the molecular and cellular mechanisms driving Fc-
78 dependent, mAb-mediated immunomodulation is therefore an important issue that will be key to
79 achieving protective immunity against severe viral infections by mAbs.
80

81 While several Fc-mediated effector functions (i.e. ADCC, ADCP, ….) have been shown to be required
82 for antibody-mediated antiviral protection (Bournazos et al., 2014, 2019; Earnest et al., 2019; Fox et
83 al., 2019; Gunn et al., 2018; Liu et al., 2017) whether and how FcγR engagement by antiviral mAbs
84 affects the immunomodulatory properties of different FcγR-expressing cells (i.e.
85 cytokines/chemokines secretion, activation markers expression, …) has been little studied. In
86 addition, the specific contribution of different FcγRs-expressing cells in the induction of vaccinal
87 effects by mAbs still remains ill-understood. These issues are all the more important to address given
88 that both virus-driven inflammation and Fc-mediated clearance of opsonized virus/infected cells by
89 immune effector cells generate multiple danger signals able to further modulate the host immune
90 response. However, multiple restrictions (i.e. technical and ethical issues, costs, …) largely limit those
91 studies in humans and non-human primates (NHP). As an alternative, *in vivo* studies in
92 immunocompetent mice infected with the Murine Leukemia Virus FrCasE allowed the identification
93 of several immunological mechanisms that drive protective immunity upon mAb therapy (Lambour et
94 al., 2016; Pelegrin et al., 2015). We have previously showed that treatment of FrCasE-infected mice
95 with the neutralizing mAb 667 (recognizing the retroviral envelope glycoprotein, expressed in virions
96 and infected cells) elicits protective adaptive antiviral immunity through the engagement of FcγRs.
97 Notably, mAbs form immune complexes (ICs) with viral determinants that enhance antiviral T-cell
98 responses through FcγR-mediated binding to dendritic cells (DCs) (Celis and Chang, 1984; Michaud
99 et al., 2010; Nasser et al., 2010; Yamamoto et al., 2009). We have recently shown a key

immunomodulatory role of neutrophils in the induction of protective humoral responses *via* the acquisition of B-cell helper functions upon engagement of FcγRs by the therapeutic mAb (Naranjo-Gomez et al., 2018). Thus, the immunomodulatory actions of mAbs rely on their Fc fragment binding to multiple FcγR-expressing cells such as DCs and neutrophils. While the role of IC-activated DCs in the enhancement of antiviral immune responses has been addressed in several studies (Lambour et al., 2016; Wang et al., 2019; Wen et al., 2016) the role of IC-activated neutrophils has mostly been overlooked. Evidence shows that neutrophils, in addition to being key effector cells to fight against invading pathogens, are also endowed with immunomodulatory properties through the secretion of a plethora of chemokines and cytokines (Mantovani et al., 2011; Tamassia et al., 2018; Tecchio and Cassatella, 2016). Yet, the functional activation of neutrophils by viral ICs and the resulting effect on their immunomodulatory properties have poorly been studied in the context of antiviral mAbs therapies. Furthermore, recent studies have highlighted a vast heterogeneity of neutrophils phenotypes and functions in both homeostatic and pathological conditions (Deniset and Kubes, 2018; Ng et al., 2019; Scapini et al., 2016; Silvestre-Roig et al., 2016, 2019). As these phenotypic and functional variants of neutrophils depend on their context-dependent stimulation (inflammatory environment, timing, disease progression, …), it is important to dissect how the viral infection and mAb therapy shape the phenotype and functional properties of neutrophils.

Here, we used the FrCasE retroviral model to address how viral infection, with or without mAb therapy, affects the phenotypical and functional activation of neutrophils. Neutrophils activated by viral determinants secreted high levels of monocytes- and neutrophils-recruiting chemokines. We have shown that the inflammatory environment resulting from the ongoing infection and mAb-treatment modulates the functional properties of neutrophils and monocytes. We have also identified two neutrophils subpopulations with distinct functional activation states that differentially participate in the induction of Th1-type responses in mAb-treated mice in collaboration with inflammatory monocytes. Our work provides hitherto unreported findings on both the heterogeneity and immunomodulatory properties of neutrophils in a context of antiviral mAb-therapy. These findings might help to improve mAb-based antiviral therapies by tailoring therapeutic interventions aiming at harnessing the immunomodulatory properties of neutrophils.

132 **RESULTS**
133
134 *Neutrophils activated by viral determinants, free or in the form of ICs, secrete high levels of*
135 *chemokines able to recruit monocytes and neutrophils*. We have previously shown a key role of
136 neutrophils in the induction of long-term protective antiviral immunity upon mAb therapy of infected
137 mice (Naranjo-Gomez et al., 2018). To better characterize the phenotypical and functional activation
138 of neutrophils by viral determinants, free or in the form of ICs, we isolated bone marrow (BM)
139 neutrophils from naive mice and stimulated them for 24h *in vitro* with free FrCasE virions or
140 opsonized with the 667 mAb (ICs) (Figure 1A). Free 667 mAb was used as control. Both, FrCasE
141 virions and ICs induced a strong activation of neutrophils as shown by a higher expression of the
142 CD11b molecule as well as an increased frequency of $CD11b^{hi}$ $CD62L^{lo}$ neutrophils (Figure 1B).
143 However, IC-mediated phenotypic activation was significantly higher.
144
145 We next assessed the functional activation of virus- and IC-stimulated neutrophils by measuring their
146 chemokines and cytokines secretion capacity. Both stimuli poorly induced the secretion of the 12
147 cytokines analyzed, with no significant differences between unstimulated neutrophils *versus* virus or
148 IC-stimulated neutrophils (Supplemental Figure 1A). This contrasted with the high secretion of IL-6
149 and TNFα pro-inflammatory cytokines observed upon lypopolisaccharide (LPS) neutrophils
150 stimulation despite similar CD11b upregulation induced by LPS and viral determinants (Supplemental
151 Figures 1B-1C). These data show that bacterial-related pathogen-associated molecular patterns
152 (PAMPs) induce a functional activation of neutrophils different from that of viral stimuli. In contrast
153 to cytokine secretion, both virus and ICs lead to high secretion levels of several chemokines such as
154 CCL2, CXCL1, CXCL5 and to a lesser extent CCL3 and CCL4 (Figure 1C). In addition, LPS-
155 stimulated neutrophils only secreted a low amount of CCL3 and CCL4 chemokines, with no secretion
156 of CCL2, CXCL1, CXCL5 chemokines thus providing further evidence of a pathogen-dependent
157 secretion profile of neutrophils (Supplemental Figure 1D). Interestingly, the chemokines which were
158 more strongly secreted by neutrophils upon viral stimuli (but not by LPS) have been shown to be
159 involved in the recruitment of monocytes (CCL2) (Fan et al., 2018; Kim et al., 2011; Leonard and
160 Yoshimura, 1990; Robben et al., 2005) and neutrophils themselves (CXCL1, CXCL5) (Haider et al.,
161 2019; Pruenster et al., 2009; Ritzman et al., 2010; Rovai et al., 1998).
162
163
164 *Inflammatory monocytes activated by viral determinants, free or in the form of ICs, secrete high levels*
165 *of chemokines able to recruit neutrophils and monocytes*. Taking into account the high amounts of the
166 monocytes-recruiting CCL2 chemokine secreted by viral determinants-activated neutrophils, we next
167 assessed the phenotypical and functional activation of monocytes by these stimuli. $Ly6C^{hi}$ monocytes
168 were isolated from naive mice BM and stimulated for 24h with virus or ICs (Figure 2A). Phenotypical
169 activation was evaluated by measuring the CD86 co-stimulatory molecule expression on the cell

170 surface. Free virions and ICs significantly increased CD86 expression but no significant differences
171 were observed between both stimuli (Figure 2B).
172
173 Virus- and ICs induced a weak secretion of most of the 12 cytokines analyzed, except for IL6 and
174 TNFα. However, no significant differences between unstimulated monocytes *versus* virus- or IC-
175 stimulated monocytes were detected (Supplemental Figure 2A). This contrasted with high level
176 secretion of IL-6, TNFα and IFNγ observed upon LPS stimulation (Supplemental Figures 2B-2D).
177 The quantification of the chemokine release by activated monocytes showed some interesting
178 similarities with neutrophils. Following virus or ICs stimulation, monocytes produced CXCL5,
179 CXCL1 and CCL2, with no significant differences between virus *versus* ICs (Figure 2C). As
180 compared to neutrophils, higher amounts of the neutrophil-recruiting chemokine CXCL1 were
181 detected as well as lower amounts of CXCL5 and CCL2. Interestingly, LPS stimulation induced a
182 wider and different panel of chemokine release (Supplemental Figure 2D), notably with the secretion
183 of high amounts of CCL3, CCL4, CCL5, and to a lesser extent CXCL1 and CXCL10. As observed in
184 neutrophils, these data show that viral stimuli induce a functional activation of monocytes different
185 from that of bacterial-related PAMPs.
186
187 *Inflammatory conditions potentiate the activation of neutrophils and monocytes by viral ICs*. As the
188 inflammatory microenvironment resulting from the viral infection and mAb therapy might affect the
189 antiviral immune response, we next assessed the phenotypic and functional activation of neutrophils
190 and monocytes by viruses and ICs in the presence of proinflammatory/immunomodulatory cytokines,
191 such as TNFα, IFN-I and IFNγ.
192
193 As depicted by an increased expression of CD11b, TNFα and IFNγ significantly enhanced the
194 phenotypic activation of neutrophils by ICs (but not by free virus) (Figure 3A). Priming conditions
195 also modulated the secretion profile of virus- and IC-activated cells in a cytokine-specific manner.
196 TNFα enhanced the secretion of CXCL1 and TNFα itself by IC-activated neutrophils but not by virus-
197 activated neutrophils (Figure 3B, Supplemental figure 3A). IFN-I and IFNγ (Figure 3B, Supplemental
198 figure 3A) significantly potentiated CCL4 secretion by IC-activated neutrophils. Both types of IFN
199 induced the production of CXCL10, consistent with the IFN-dependent induction of this chemokine.
200 However, CXCL10 secretion was significantly increased in neutrophils activated by virus or ICs upon
201 IFN priming. IFNγ also significantly enhanced CCL5 and CXCL1 secretion by IC-stimulated
202 neutrophils. In contrast, TNFα-, IFN-I- or IFNγ priming did not modulate the secretion of CCL2,
203 CXCL5 and CCL3 by neither virus- nor IC-activated neutrophils (not shown).
204

205 As for monocytes, IFN-I and IFNγ significantly potentiated the phenotypic activation of IC-stimulated
206 monocytes (as depicted by an increased expression of CD86 molecule) (Figure 3C) but not that of
207 virus-activated cells. TNFα, IFN-I or IFNγ significantly potentiated the secretion of CCL2 and
208 CXCL1 (Figures 3D and Supplemental figures 3B) by IC-activated monocytes. Similar to neutrophils,
209 IFNγ and IFN-I enhanced the secretion of CXCL10 by IC-stimulated monocytes and IFN-I
210 significantly increased the production of TNFα. Priming conditions also modulated the
211 cytokine/chemokine secretion profile of virus-activated monocytes, but in a more restricted way than
212 in IC-activated cells. Thus, CXCL1 secretion was enhanced by TNFα and IFNγ and CCL2 by IFN-I.
213 Both types of IFN also increased the release of CXCL10 by virus-activated monocytes (Figure 3D).
214 Similar secretion levels of CXCL5 virus- and IC-activated monocytes were observed in the presence
215 or in the absence of TNFα-, IFN-I- and IFNγ- priming (not shown).
216
217 Altogether, these data highlight that inflammatory conditions strongly potentiate the functional
218 activation of IC-stimulated neutrophils and monocytes, although with different immune outcomes
219 depending on the priming condition and the responding cell type (Figure 3). Our data describe a
220 distinct enhancement of neutrophils and monocytes secretion profile by TNFα-, IFN-I- and IFNγ-
221 priming showing thus a cytokine-specific effect on the functional activation of these IC-stimulated
222 cells. Such cytokine/chemokine secretion enhancement is also cell type specific (i.e. increased
223 secretion of CCL4, CCL5, CXCL1 and TNFα by IC-activated neutrophils and CCL2, CXCL1 and
224 TNFα by IC-activated monocytes). In contrast, inflammatory conditions hardly modify the secretion
225 profile of free virus-activated cells, except for the secretion of the CXCL10 IFN-inducible chemokine.
226
227 *Inflammatory conditions upregulate the expression of FcγRIV on in vitro activated neutrophils and*
228 *monocytes*. We next assessed whether the activation of neutrophils and monocytes by virus and IC
229 affected their FcγRs expression, both in the absence and in the presence of inflammatory cytokines.
230 Indeed, FcγRs expression might differ between steady-state *versus* inflammatory/pathological
231 conditions (Wang and Jönsson, 2019), however little is known about modulation of FcγRs expression
232 in the context of viral infections and mAb-therapy. Neither virus nor IC upregulated the expression of
233 FcγRIV on neutrophils and monocytes (Figure 4A-4D). On the contrary, IFNγ and IFN-I priming (but
234 not TNFα) upregulated the expression of FcγRIV on neutrophils (IFNγ) (Figure 4B) and monocytes
235 (IFNγ and IFN-I) (Figure 4D). Both IFNs also enhanced FcγRI expression on monocytes whereas a
236 decreased FcγRII-III expression was observed following IC stimulation and cytokine-priming
237 (Supplemental Figure 4). No FcγRI expression was detected on neutrophils neither upon viral
238 determinants stimulation nor cytokine priming.
239

240 *Viral infection and mAb therapy upregulate FcγRIV expression on two neutrophils subpopulations and*
241 *on inflammatory monocytes*. We next assessed *in vivo* whether the inflammatory environment
242 resulting from FrCasE viral infection and 667 mAb therapy modulated the expression of FcγRIV. The
243 modulation of this FcγR is all the more relevant to be studied in this experimental model as (i) it is a
244 high affinity receptor for IgG2a, (which is the isotype of the 667 mAb) and (ii) it is strongly expressed
245 in neutrophils, the latter having a key immunomodulatory role in mAb-mediated protection of
246 retrovirus-infected mice (Naranjo-Gomez et al., 2018).
247
248 To this end, mice were infected and treated, or not, with the therapeutic mAb (infected/treated and
249 infected/non-treated, respectively). Then, the expression of FcγRIV on neutrophils and inflammatory
250 monocytes from the spleen (one of the main sites of viral replication) was evaluated at different time
251 points post-infection (p.i.). Age-matched naive mice were used as controls. The cell populations of
252 interest were defined by flow cytometry (Figure 5A) based on the expression of CD11b, Ly6G and
253 Ly6C to gate neutrophils ($CD11b^{+}$, $Ly6G^{hi}$) and inflammatory monocytes ($CD11b^{+}Ly6G^{-}Ly6C^{hi}$).
254 Interestingly, we identified another population of neutrophils displaying a lower expression of the cell
255 surface marker Ly6G ($CD11b^{+}Ly6G^{int}$) (Figure 5A). No expression of the eosinophils cell surface
256 marker Siglec F was detected in this population (not shown). The frequency of both populations of
257 neutrophils $CD11b^{+}Ly6G^{hi}$ and $CD11b^{+}Ly6G^{int}$ was significantly increased in the spleen of
258 infected/non-treated mice at 8 and 14 days p.i. This increased neutrophil frequency was associated
259 with a higher percentage of spleen infected cells as compared to infected/treated mice (Naranjo-
260 Gomez et al., 2018). On the contrary, the frequency of inflammatory monocytes ($CD11b^{+}Ly6G^{-}$
261 $Ly6C^{hi}$) remained unchanged in infected mice at day 8 p.i. but was significantly increased at day 14
262 p.i. (Figure 5B), suggesting an earlier recruitment of neutrophil than inflammatory monocytes upon
263 infection.
264
265 In steady-state conditions, FcγRIV was highly expressed on $CD11b^{+}Ly6G^{hi}$ and $CD11b^{+}Ly6G^{int}$
266 neutrophils. Lower FcγRIV expression was detected in inflammatory monocytes at the different time
267 points assessed (Figure 5C). Notably, upon viral infection and mAb-treatment, FcγRIV expression was
268 upregulated in the three myeloid cells populations although, to a different magnitude depending on the
269 cell type, time p.i. and mAb-treatment (Figure 5C). At day 8 p.i. FcγRIV expression was significantly
270 upregulated on neutrophils and monocytes in infected/treated and infected/non-treated mice, the latter
271 showing a stronger FcγRIV upregulation. In contrast, at day 14 p.i. infected/treated mice showed a
272 stronger upregulation of FcγRIV on the three myeloid cells populations as compared to infected/non-
273 treated and control mice. $CD11b^{+}Ly6G^{int}$ neutrophils displayed the strongest expression of FcγRIV as
274 well as the highest magnitude of FcγRIV upregulation after infection and mAb-treatment. No
275 detectable FcγRI expression was observed at day 8 p.i. in any of the three cell types assessed.

However, at day 14 p.i. infected/treated mice showed a significant upregulation of this inducible FcγR receptor in CD11b^{+}Ly6G^{int} neutrophils and monocytes (Supplemental Figure 5).

These results highlight that viral infection and mAb therapy results in an evolving inflammatory environment that dramatically modulates the expression of FcγRs in neutrophils and monocytes, leading to a stronger upregulation of FcγRIV at 8 days p.i. in infected/non treated mice and at 14 days p.i. in infected/treated mice.

High Fc*γRIV-expressing CD11b^{+}Ly6G^{int} neutrophils subpopulation displays phenotypic properties different from those of CD11b^{+}Ly6G^{hi} neutrophils*. High level expression and strong upregulation of FcγRIV on CD11b^{+}Ly6G^{int} (Figure 5C and 5D) suggested different and specific properties of this neutrophil subpopulation. We thus characterized it further. We observed neutrophils Ly6G^{int} to be smaller than neutrophils Ly6G^{hi} and displaying a lower granulosity (Figure 5D). To determine the specificities of this population, we studied the expression pattern of neutrophils and monocytes cell-surface markers in these cells at steady-state conditions (Figure 5E). Similar to CD11b^{+}Ly6G^{hi} neutrophils, CD11b^{+}Ly6G^{int} cells expressed low levels of the monocyte cell surface markers Ly6C and CCR2 (Figure 5E). They also expressed the CXCR4 chemokine receptor although at intermediate levels as compared to CD11b^{+}Ly6G^{hi} neutrophils and inflammatory monocytes. However, they weakly express the chemokine receptor CXCR2 which is highly expressed on CD11b^{+}Ly6G^{hi} neutrophils.

These results revealed that Ly6G^{int} cells display a neutrophil-like phenotype but with specific characteristics as compared to classical Ly6G^{hi} neutrophils, notably (i) smaller size and granulosity, (ii) higher viral-induced FcγRIV expression, and (iii) a pattern expression of cell surface markers characteristic of neutrophils (Ly6C^{lo}, CCR2^{-}, CXCR4^{int}) except for the lack of expression of the CXCR2 receptor. This suggests that CD11b^{+}Ly6G^{int} cells are a phenotypic variant of neutrophils. However, whether CD11b^{+}Ly6G^{int} cells represent a *bona fide* novel neutrophils subset or neutrophils displaying a different activation/maturation state could not be discriminated by these phenotypic properties as this will require integrative high-dimensional analyses including not only functional and phenotypic characterization but also deep genomic profiling of the neutrophil subpopulations identified (Ng et al., 2019).

FcγRIV upregulation in infected/treated mice is associated with enhanced expression of MHC-II and co-stimulatory molecules on neutrophils and monocytes. We next addressed *in vivo* the functional activation of splenic neutrophils and inflammatory monocytes in infected mice with or without immunotherapy at days 8 and 14 p.i. by monitoring cell surface activation markers. We were able to

312 show that the activation state of the cells evolved over time. At day 8 p.i., (Figure 6A) CD11b was
313 upregulated on neutrophils and monocytes upon viral infection either in the absence or in the presence
314 of immunotherapy. However, infected/treated mice showed a significantly higher CD86 upregulation
315 in CD11b^{+}Ly6G^{hi} and CD11b^{+}Ly6G^{int} neutrophils than infected/non-treated mice. MHC-II molecule
316 was also upregulated on CD11b^{+}Ly6G^{int} neutrophils and monocytes upon viral infection. At day 14 p.i.
317 (Figure 6B), CD11b^{+}Ly6G^{hi} splenic neutrophils were similarly activated in infected/treated- and
318 infected/non-treated mice, as deduced from an increased expression of CD11b and CD86. However,
319 CD86 expression on CD11b^{+}Ly6G^{int} neutrophils was significantly increased in infected/treated mice,
320 suggesting a mAb-mediated upregulation of these costimulatory molecules on this neutrophil
321 subpopulation. Likewise, inflammatory monocytes from infected/treated mice also showed a
322 significantly increased expression of CD86 co-stimulatory molecules as compared to infected/non-
323 treated mice. Notably, MHC-II expression was significantly increased in infected/treated mice in both
324 neutrophil populations as well as in monocytes as compared to infected/non-treated mice.
325
326 Consistent with a FcγRIV upregulation in neutrophils and monocytes in infected/treated mice (Figure
327 5C), these data demonstrate a mAb-mediated upregulation of MHC-II and costimulatory molecules in
328 CD11b^{+}Ly6G^{int} neutrophils and monocytes as well as a significant upregulation of MHC-II in
329 CD11b^{+}Ly6G^{hi} neutrophils at 14 days p.i. (Figure 6B).
330
331
332 *CD11b^{+}Ly6G^{hi}, CD11b^{+}Ly6G^{int} neutrophils and inflammatory monocytes are differentially and*
333 *sequentially activated upon antiviral mAb treatment*. To further characterize the functional activation
334 state of the two neutrophils populations (CD11b^{+}Ly6G^{hi} and CD11b^{+}Ly6G^{int}) and inflammatory
335 monocytes upon viral infection and mAb-therapy, we next addressed the cytokine and chemokine
336 secretion profile of splenic neutrophils and monocytes sorted from infected mice treated, or not, with
337 the 667 mAb, at days 8 and 14 p.i. Cells sorted from age-matched naive mice were used as controls.
338 We found that the secretion profile evolved over time and was cell type- and stimulus specific, with
339 globally enhanced cytokine/chemokines secretion in cells isolated from infected/treated mice (Figure
340 7A and 7B), in particular at day 14 p.i.
341
342 At day 8 p.i., the CD11b^{+}Ly6G^{hi} neutrophils subpopulation from both infected/non-treated and
343 infected/treated mice showed a broad chemokine and cytokine secretion profile as deduced from an
344 increased secretion of most of the 13 chemokines and 12 cytokines assessed, although at weak levels
345 (Figure 7B and 7C). CD11b^{+}Ly6G^{int} neutrophils showed enhanced expression of several chemokines
346 mostly in cells isolated from infected/non-treated mice notably with a strong enhanced secretion of
347 CCL3, CCL5 and CXCL5. In addition, CD11b^{+}Ly6G^{int} neutrophils also showed a slight secretion of
348 multiples cytokines in infected/treated mice, but to a lesser extent than CD11b^{+}Ly6G^{hi} neutrophils

349 (lower fold-increase) (Figure 7B and 7C). In contrast, infection and mAb-treatment hardly affected the
350 chemokine/cytokine secretion of Ly6C^{hi} monocytes. They only showed a weak increase in CXCL1
351 secretion in infected/treated mice as well as a slight increase in cytokines secretion (both in terms of
352 diversity and fold increase) mainly in infected/non-treated mice (Figure 7B).
353
354 Interestingly, at day 14 p.i., the functional activation of the three different cell types assessed
355 completely differed from that observed at day 8 p.i. (Figure 7B and 7C). We found a more restricted
356 but stronger induction of chemokines/cytokines secretion, mostly in cells isolated from
357 infected/treated mice. In contrast to the broad cytokines and chemokines secretion profile observed at
358 day 8 p.i., CD11b^{+}Ly6G^{hi} neutrophils only secreted CCL4 and CCL5 chemokines and showed no
359 cytokine secretion at day 14 p.i. In addition, CD11b^{+}Ly6G^{int} neutrophils showed a strong enhanced
360 expression of 6 chemokines (CCL3, CCL4, CCL5, CCL22, CXCL9 and CXCL10) and 3 Th1-
361 polarizing cytokines (IL-6, TNFα, IFNγ) in infected/treated mice. Ly6C^{hi} monocytes showed a
362 proinflammatory chemokine/cytokine secretion profile similar to CD11b^{+}Ly6G^{int} neutrophils, except
363 for the secretion of CXCL9, that was specific to CD11b^{+}Ly6G^{int} neutrophils and CXCL1 that was only
364 secreted by monocytes.
365
366 In summary, FrCasE infection and 667 mAb-treatment induce the secretion of multiple chemokines
367 and cytokines by neutrophils and monocytes. Interestingly, the secretion profile evolves over time and
368 differs among the three different cell types assessed, providing further evidence of a different
369 functional activation state of the two neutrophils subpopulations (Ly6G^{hi} and Ly6G^{int}). In addition,
370 these data show an enhanced secretion of Th1-polarizing cytokines and chemokines by cells isolated
371 from infected/treated mice at 14 p.i, showing a role for the therapeutic mAb in the functional
372 activation of these FcγRIV highly-expressing cells.
373

374 **DISCUSSION**
375

376 We have previously shown that neutrophils have a key immunomodulatory role in the induction of
377 protective immunity by antiviral mAbs through the acquisition of B-cell helper functions (Naranjo-
378 Gomez et al., 2018). Here we provide a new insight into both the heterogeneity and
379 immunomodulatory role of neutrophils in a context of antiviral mAb-therapy. Our work shows that
380 two functionally distinct neutrophil subpopulations can secrete multiple cytokines and chemokines
381 able to recruit and activate multiple cells of the innate and the adaptive immune system. The
382 cytokine/chemokine secretion profile: differs between both neutrophil subpopulations, is stimulus-
383 dependent, evolves over time upon viral infection and mAb-treatment and suggests a potential
384 cooperation with inflammatory monocytes in the induction of Th1 immune responses upon mAb-
385 treatment of infected mice.
386

387 Our data show that neutrophils cytokine/chemokine secretion profile differs between viral *versus*
388 bacterial stimulus. This is important to highlight as most of the studies investigating the
389 immunomodulatory role of neutrophils have been conducted in bacterial infection models. Thus, *in*
390 *vitro* stimulation of neutrophils by viral determinants led to a poor production of cytokines but to a
391 wide and strong release of chemokine, with notably high secretion levels of the monocytes-and
392 neutrophils-recruiting chemokines (CCL2, CXCL1, CXCL5) that was not observed upon LPS
393 stimulation. On the contrary, LPS-stimulated neutrophils produced high amounts of proinflammatory
394 cytokines but a narrower and weaker chemokine release. As for neutrophils, stimulation of monocytes
395 by viral determinants (but not LPS) led to the secretion of high amounts of the neutrophils-recruiting
396 chemokine CXCL1 and to a lesser extent the monocytes-recruiting chemokine CCL2. These results
397 suggest a self-sustaining mechanism of neutrophils and monocytes recruitment upon viral infection,
398 and raise the hypothesis of an early cooperation between neutrophils and monocytes in the
399 modulation/induction of the antiviral immune response. This secretion profile of neutrophils induced
400 by viral determinants is in agreement with an increased CCL2 release observed upon *in vitro* HIV
401 stimulation of neutrophils (Yoshida et al., 2009). Increased levels of CCL2 and CXCL1 have also
402 been reported in neutrophil- and monocytes-infiltrated tissues in different viral infections, (Hokeness
403 et al., 2005; Miller et al., 2004; Rubio and Sanz-Rodriguez, 2007; Seo et al., 2011). However,
404 chemokine increase was mostly assessed in total tissue extracts but not directly in neutrophils or
405 monocytes isolated cells, which prevented the identification of the cell origin of chemokines. It is
406 worth noting that a very early but transient expression has also been reported (i.e. 24-48h p.i.) of
407 CCL2 and CXCL1 upon infection by RSV, CMV and influenza virus (Hokeness et al., 2005; Miller et
408 al., 2004; Wareing et al., 2004). Such early and transient expression would be in agreement with the
409 very low secretion of these chemokines detected at day 8 p.i. in infected mice treated, or not, with the
410 therapeutic mAb.

411

412 Our data also highlight the effect of inflammatory conditions on the modulation of the phenotypic and
413 functional activity of neutrophils and monocytes. Thus, *in vitro* priming with
414 inflammatory/immunomodulatory cytokines clearly potentiated the release of several chemokines and
415 cytokines by IC-activated neutrophils and monocytes (Figure 3) while having a less pronounced or no
416 effect on virus-activated cells. This suggests that cytokine-priming associated to FcγR-triggering leads
417 to enhanced immune responses. Although not formally shown, these results support a role for the
418 inflammatory environment in the enhancement of chemokine/cytokine secretion by neutrophils and
419 monocytes observed in infected-treated mice. Furthermore, our *in vitro* observations also allowed us to
420 dissect the specific effect of IFN-γ, IFN-I and TNF-α on the enhancement of the functional properties
421 of IC-activated neutrophils and monocytes. Notably, IFN-γ and IFN-I priming (but not TNF-α), led to
422 the upregulation of FcγRs in neutrophils and/or monocytes, in agreement with previous reports in
423 other experimental settings (Dahal et al., 2017; Lehmann et al., 2017; Morquin et al., 2017; Pricop et
424 al., 2001). Consistent with these results, our *in vivo* work shows that the inflammatory environment
425 resulting from ongoing infection and mAb-treatment also modulates FcγRs expression on neutrophils
426 and monocytes (in particular FcγRIV). Thus, FcγRIV expression is more strongly enhanced in
427 infected/non-treated mice at day 8 p.i. and in infected/treated mice at day 14 p.i., suggesting a different
428 and evolving inflammatory environment in both groups of mice. These results are in agreement with
429 previous work showing FcγRs modulation by the inflammatory conditions resulting from bacterial and
430 IC-mediated autoimmune pathologies (Bruhns, 2012; Wang and Jönsson, 2019); and provide new
431 evidence on the regulation of FcγRs expression in the specific inflammatory context of antiviral mAb-
432 based immunotherapies, not hitherto reported. Notably, our work shows that the magnitude of FcγRIV
433 upregulation upon viral infection and mAb-treatment is different in neutrophils and monocytes. This
434 differential FcγRIV expression together with a different expression level of the Ly6G neutrophil cell
435 surface marker ($Ly6G^{hi}$ and $Ly6G^{int}$) contributed to the identification and characterization of two
436 neutrophils subpopulation displaying distinct functional properties as deduced from their different (i)
437 phenotype (size, granulosity, cell surface molecules) (Figures 5 and 6), (ii) magnitude of expression
438 and upregulation of FcγRIV, costimulatory molecules and MHC-II (Figures 5 and 6) and (iii)
439 cytokine/chemokine secretion profile (Figure 7) upon viral infection and mAb-treatment. Recent
440 studies have shown neutrophils heterogeneity in healthy tissues as well as in different pathological
441 conditions (Ng et al., 2019; Silvestre-Roig et al., 2019) through the identification of different
442 neutrophils subpopulations. Such neutrophil heterogeneity is context-dependent as it is influenced by
443 the nature and magnitude of the stimuli. In the particular context of infectious diseases, neutrophils
444 heterogeneity is still poorly characterized and it has mostly been assessed in bacterial infections
445 (Deniset et al., 2017; Tsuda et al., 2004). Similar to our observations Deniset and collaborators
446 (Deniset et al., 2017) reported two distinct splenic neutrophils subpopulations displaying different

447 Ly6G expression levels (Ly6G^{hi} and Ly6G^{int}) in *Streptococcus pneumoniae* infected mice. This study
448 evidenced some phenotypic differences (cell surface markers of maturation, nuclear morphology, ….)
449 between both neutrophil subpopulations but their functional activation was not assessed. Importantly,
450 we describe here two phenotypic and functional variants of neutrophils displaying distinct
451 immunomodulatory properties that might be key and complementary for inducing antiviral protective
452 immunity. Our work provides thus novel findings on the heterogeneity and function of neutrophils
453 upon viral infection and mAb-treatment.
454
455 Our work provides new mechanistic insights into the hitherto underestimated role of neutrophils as
456 key cells in the modulation of adaptive antiviral immunity upon mAb treatment. Interestingly, at
457 steady-state conditions, neutrophils express high levels of FcγRIV. Its expression is higher than that
458 observed in inflammatory monocytes. Thus, it is tempting to speculate that upon viral infection and
459 mAb-treatment, the early neutrophils recruitment, together with their high expression of FcγRIV,
460 result in potent Fc-triggering by ICs in these cells. This might be key to initiate the modulation of
461 immune responses through the production of multiple cytokines and chemokines able to recruit and
462 activate multiple innate immune cells such as monocytes, NK cells, DC and neutrophils themselves
463 (Tecchio and Cassatella, 2016). This suggest a potential role for neutrophils as early drivers of the
464 induction of vaccinal effects by mAbs. Supporting this hypothesis, at day 8 p.i. both neutrophils
465 populations showed a higher and a wider induction of chemokines and cytokines release than
466 monocytes. Subsequently, the inflammatory environment resulting from viral infection and mAb-
467 mediated antiviral effects induces the upregulation of FcγRs in the different innate immune cells that
468 might further increase Fc-triggering by ICs leading to improved immune responses, both in terms of
469 magnitude and quality. In agreement with this, the FcγRIV upregulation in neutrophils and monocytes
470 in infected/treated mice observed at 14 days p.i. is associated with (i) higher expression of
471 costimulatory molecules and MHC-II and (ii) higher secretion of cytokines and chemokines. In
472 keeping with this, enhanced secretion of Th1-polarizing cytokines (IL-6, TNFα, IFNγ) (Czarniecki,
473 1993; Hildenbrand et al., 2008; Jin et al., 2016; Uciechowski and Dempke, 2020; Wang et al., 2005)
474 and chemokines (CXCL9 and CXCL10) (Gaylo-Moynihan et al., 2019; Kelly-Scumpia et al., 2010;
475 Tannenbaum et al., 1998; Tokunaga et al., 2018) by CD11b^{+}Ly6G^{int} neutrophils and monocytes from
476 infected/treated mice at 14 p.i, argues in favor of a mAb-mediated Th1 polarization of the antiviral
477 immune response by these cells. Consistent with such Th1 polarization, we previously reported strong
478 CD8 T-cells responses at day 14 p.i. in infected/treated mice (Gros et al., 2008; Michaud et al., 2010)
479 as well as long-lasting protective humoral immune responses predominantly of the IgG2a isotype
480 (Gros et al., 2005; Michaud et al., 2010; Naranjo-Gomez et al., 2018). Finally, it is also worth
481 mentioning the upregulation of MHC-II molecules observed in CD11b^{+}Ly6G^{hi} and CD11b^{+}Ly6G^{int}
482 neutrophils sorted from infected/treated mice. This observation broadens the immunomodulatory role

483 of neutrophils upon mAb-treatment as it suggests that neutrophils might acquire antigen-presenting
484 cell features and induce antigen-specific T-cells responses (Lok et al., 2019; Meinderts et al., 2019;
485 Vono et al., 2017). In agreement with this, it has been shown that upon *ex vivo* stimulation with IgG
486 immune complex (IC) or viral cognate antigens, neutrophils upregulated expression of MHCII and
487 costimulatory molecules and increased T cell activation.
488
489 Our work show that mAb-mediated activation of neutrophils and monocytes might be essential to
490 induce strong Th1-polarized early immune responses that might be key to induce protective immunity
491 by mAb. In addition, the distinct secretion profile of Ly6G^{hi} and Ly6G^{int} neutrophils and Ly6C^{hi}
492 monocytes, in terms of type, amount and kinetics of chemokines/cytokines secretion, shows a
493 differentially and sequentially activation of theses FcγRIV-expressing cells upon antiviral mAb
494 treatment and suggests their key and complementary action in the induction of protective immune
495 responses by mAb. Thus, the identification of neutrophils as key players in the induction of protective
496 immunity by antiviral mAbs and their potential collaboration with inflammatory monocytes might
497 have therapeutic implications. These findings might help to improve mAb-based antiviral therapies by
498 tailoring therapeutic interventions aiming at harnessing the immunomodulatory properties of these
499 cells. To this end, different approaches could be envisaged: (i) the use of appropriate
500 immunostimulatory host-directed therapies and (ii) the design of antiviral mAbs engineered to
501 enhance their affinity for FcγRs expressed on human neutrophils and monocytes, such as FcγRIIa and
502 FcγRIIIa (Bournazos et al., 2019; Chen et al., 2017; DiLillo and Ravetch, 2015) .Thus, in addition to
503 allow superior antibody-mediated phagocytosis, these Fc-engineered mAbs could also modulate
504 cytokine/chemokine production to ultimately lead to more effective adaptive immune responses.
505
506
507

508 **METHODS**
509

510 ***Mice:*** Inbred 129/Sv/Ev mice (H-2D^b haplotype) were used and maintained under conventional,
511 pathogen-free facilities at the Institut de Génétique Moléculaire de Montpellier (RAM-ZEFI). They
512 have been used without distinction as to sex and at different ages according to experiments.

513 ***Viral stocks***: FrCas^E (Portis et al., 1990) viral stocks were produced and stored as previously
514 described in (Gros et al., 2005).

515 ***Viral infection and immunotherapy:*** Eight-day-old 129/Sv/Ev mice were infected by
516 intraperitoneal (i.p.) administration with 50 µl of a viral suspension containing 50,000 focus-forming
517 units (FFU) and treated, or not, with 30 µg 667 mAb targeting gp70 protein of viral envelope,
518 (McAtee and Portis, 1985), 1-hour p.i. and on days 2 and 5 p.i. by i.p. administration. Mice were
519 euthanized and spleens collected at days 8 and 14 p.i.
520

521 ***Phenotypical and functional activation of FcγRIV-expressing cell from spleen ex vivo:***
522 Single-cell suspensions of splenocytes were obtained from naive, infected/non-treated and
523 infected/treated mice at 8 and 14 days p.i. and immunotherapy. Spleen cell suspensions were obtained
524 by mechanical dissociation in PBS, then filtered in 0,70 μm strainer. 20 % of each spleen was used for
525 immunophenotyping by FACS, 80% left was dedicated to main FcγRIV-expressing cell sorting. Red
526 blood cells were lysed (ACK, Lonza) and an enrichment with biotinylated anti-B220 (BD
527 Biosciences), anti-CD3 (BD Biosciences), following of anti-biotin Ab magnet-bead coupled
528 (Miltenyi) and magnetic LS-columns (Miltenyi) was performed to remove spleen lymphocytes and
529 increase the sorting efficacy. Cells were stained with specific marker of populations of interest (Ly6G-
530 BD BioSciences, Ly6C-BioLegend, CD11b-BD BioSciences) and neutrophils (Ly6G^{hi} and L6G^{int}) and
531 inflammatory monocytes (Ly6C^{hi}) were sorted (>97-98% pure) using the BD Biosciences FACSAria
532 device. Sorted cells were cultured in 96-well plates at a density of 4x10^6 cells/ml (1x10^6 cells/well) in
533 10% FBS-containing RPMI medium for 24h, and cell-free supernatants were collected and stored at -
534 20°C, to allow cytokines and chemokines protein release quantification.

535 ***Flow cytometry:*** Organs of interest were collected to realize immunophenotyping of immune cells.
536 Spleen cell suspensions were obtained by mechanical dissociation in PBS. BM cell suspensions were
537 obtained by dissection and PBS-2%-FBS flushing of tibias and femurs. Cells were stained at 4°C
538 using fluorochrome-conjugated antibodies against CCR2 (SA203G11, BioLegend), CD11b (M1/70,
539 eBioscience), CD11c (HL3, BD Biosciences), CD16/32 (93, BD Biosciences), CD45.2 (104, BD
540 Biosciences), CD62L (MEL-14, BD Biosciences), CD64 (x54-5/7.1, BD Biosciences), CD86 (GL1,
541 BD Biosciences), CXCR2 (SA044G4, BioLegend), CXCR4 (2B11, Life Technologies), Ly6G (1A8,

542 BD Biosciences), Ly6C (AL-21, BioLegend) and Siglec F (E50-2440, BD Pharmingen). FcγRIV
543 expression was determined using 9E9 antibody (kindly provided by Dr.Pierre Bruhns, Institut
544 Pasteur), produced by BioXcell, and then labeled with Alexa Fluor 647. FrCasE-infected cells were
545 assayed using an anti-Gag mAb (H34) (Chesebro et al., 1981; kindly provided by Pr. Ulf Dittmer,
546 University of Duisburg-Essen) labeled with Alexa Fluor 647 or incubated with an anti-IgG2b labeled
547 PE. Forward scatter area and forward scatter time-of-flight, as well as side scatter, were used to
548 remove doublets from flow cytometry analyses. Cells were analyzed on FACS LSR Fortessa (BD
549 Bioscience), and the data were analyzed using the FlowJo software.

550 ***Neutrophils and monocytes isolated from BM used in in vitro experiments:*** Neutrophils and
551 monocytes were purified from 8 to 11-week-old naive mice BM. After dissection of lower limbs, BM
552 cell suspensions were collected by PBS-2% FBS EDTA (2 mM) flushing (25G needle) of tibias and
553 femurs. BM cell suspensions were filtered with a 0,40 μm nylon strainer. Two magnetic-based cell
554 sorting (MACS) isolation kits were used to purified either neutrophils (Miltenyi Biotec) and
555 monocytes, (Miltenyi Biotec), both with high purity (>97-98%), determined by FACS (LSR Fortessa,
556 BD Bioscience). Cells were placed in culture in U bottom 96-well plates at a concentration of 1
557 million/ml in 10% FBS-containing RPMI medium.
558
559 ***Stimulation of neutrophils and monocytes in vitro***: Purified neutrophils and monocytes were
560 seeded at 150 000 cells/ well in 150 μl of RPMI, then incubated for 24h with LPS (1μg/ml, Sigma), or
561 $FrCas^E$ virus (MOI 5: 5 viral particles /cell), or ICs (virus $FrCas^E$ and 1μg 667 mAb), or 1μg 667 mAb
562 alone. In parallel, the same experiments were performed adding inflammatory cytokines, TNFα 100
563 UI/ml (Peprotech), IFN γ 100 UI/ml (eBioScience), IFNα11 a 1000 UI/ml, produced and generously
564 provided by Dr. Gilles Uzé (DIMP, CNRS). After 24h of stimulation, supernatants were collected and
565 stored at -20°C to quantify chemokines and cytokines protein release secretion (describe below).
566 Phenotypical activation of both neutrophils and monocytes was measured using surface markers by
567 flow cytometry.
568
569 ***Chemokines and cytokines protein release quantification:*** Soluble chemokines and cytokines
570 secretion were quantified from cell-free collected supernatants of *in vitro* cultured neutrophils and
571 monocytes and of sorted splenic neutrophils $Ly6G^{hi}$ and $Ly6G^{int}$, and inflammatory monocytes (of
572 naive, infected/non-treated and infected/treated mice 8 and 14 days p.i. and immunotherapy), using
573 bead-based immunoassays (LegendPLex, BioLegend) and analyzed on the BD Bioscience-LSR
574 Fortessa device. The protein release quantification was established by the appropriate software
575 (LEGENDplex™ data analysis).

576 ***Statistics:*** Statistical analyses were performed using GraphPad Prism 5 (GraphPad Software). Data
577 were expressed as mean ± SEM, and statistical significance was established using a parametric 1-way
578 ANOVA test or non-parametric Kruskal-Wallis test for multiple comparisons or paired Student's *t*
579 tests when two groups were compared. *P* values lower than 0.05 were considered as statistically
580 significant.

581 ***Study approval***. All experimental procedures were performed in accordance with the French national
582 animal care guidelines (CEEA-LR-12146 approval, Ethics committee of the Languedoc-Roussillon
583 Region, Montpellier).

584

585 **AUTHOR CONTRIBUTIONS**

586
587 Jennifer Lambour (JL), Mar Naranjo-Gomez (MN-G) and Mireia Pelegrin (MP) defined the research
588 program. JL, MN-G, and Myriam Boyer-Clavel (MB-C) performed the experiments. JL, MN-G and
589 MP carried out the data analyses. JL and MP wrote the manuscript. Grants to MP funded the study.
590

591 **ACKNOWLEDGMENTS**
592

593 This work was supported by grants from the ANRS (France REcherche Nord&sud Sida-hiv
594 Hépatites), the Ligue Régionale Contre le Cancer, Sidaction and the Fondation pour la Recherche
595 Médicale. M. Naranjo-Gomez, J. Lambour, and M. Pelegrin are members of the "MabImprove
596 Labex", a public grant overseen by the French National Research Agency (ANR) as part of the
597 "Investments for the future" program (reference: ANR-10-LABX -53-01) that also supported this
598 work. We thank the imaging facility MRI, which is part of the UMS BioCampus Montpellier and a
599 member of the national infrastructure France-BioImaging, supported by the French National Research
600 Agency (ANR-10-INBS-04, "Investments for the future"). We are grateful to the animal facility of the
601 Institut de Génétique Moléculaire de Montpellier (RAM-ZEFI) which is part of the "Réseau des
602 Animaleries Montpelliéraines" RAMIBiSA Facility for animal experiments. We are grateful to S.
603 Gailhac from MRI for support in cytometry experiments, to Thierry Gostan (SERENAD Complex
604 Biological Data Analysis Service) for support in statistical analyses, to Helen Phillips Bevis for
605 English editing services and to Drs. Valerie Dardalhon, Gilles Uzé and Pascale Plence for critical
606 reading of the manuscript.
607

608 **CONFLICT OF INTEREST DISCLOSURES**
609
610 The authors declare no competing financial interests.

611 **REFERENCES**

612 Bournazos, S., and Ravetch, J.V. (2017). Fcγ Receptor Function and the Design of Vaccination
613 Strategies. Immunity *47*, 224–233.

614 Bournazos, S., Klein, F., Pietzsch, J., Seaman, M.S., Nussenzweig, M.C., and Ravetch, J.V. (2014).
615 Broadly Neutralizing Anti-HIV-1 Antibodies Require Fc Effector Functions for In Vivo Activity. Cell
616 *158*, 1243–1253.

617 Bournazos, S., DiLillo, D.J., Goff, A.J., Glass, P.J., and Ravetch, J.V. (2019). Differential
618 requirements for FcγR engagement by protective antibodies against Ebola virus. Proc Natl Acad Sci
619 USA *116*, 20054–20062.

620 Bruhns, P. (2012). Properties of mouse and human IgG receptors and their contribution to disease
621 models. Blood *119*, 5640–5649.

622 Celis, E., and Chang, T.W. (1984). HBsAg-serum protein complexes stimulate immune T
623 lymphocytes more efficiently than do pure HBsAg. Hepatology *4*, 1116–1123.

624 Chen, T.F., Sazinsky, S.L., Houde, D., DiLillo, D.J., Bird, J., Li, K.K., Cheng, G.T., Qiu, H., Engen,
625 J.R., Ravetch, J.V., et al. (2017). Engineering Aglycosylated IgG Variants with Wild-Type or
626 Improved Binding Affinity to Human Fc Gamma RIIA and Fc Gamma RIIIAs. Journal of Molecular
627 Biology *429*, 2528–2541.

628 Chesebro, B., Collins, J.K., Wehrly, K., Nishio, J., and Cloyd, M. (1981). Expression of cell surface
629 Friend virus gp70 does not block reinfection by ecotropic murine leukemia viruses. Virology *115*,
630 125–129.

631 Czarniecki, C.W. (1993). The role of tumor necrosis factor in viral disease. Antiviral Research *22*,
632 223–258.

633 Dahal, L.N., Dou, L., Hussain, K., Liu, R., Earley, A., Cox, K.L., Murinello, S., Tracy, I., Forconi, F.,
634 Steele, A.J., et al. (2017). STING Activation Reverses Lymphoma-Mediated Resistance to Antibody
635 Immunotherapy. Cancer Res *77*, 3619–3631.

636 Deniset, J.F., and Kubes, P. (2018). Neutrophil heterogeneity: Bona fide subsets or polarization states?
637 J. Leukoc. Biol. *103*, 829–838.

638 Deniset, J.F., Surewaard, B.G., Lee, W.-Y., and Kubes, P. (2017). Splenic Ly6Ghighmature and
639 Ly6Gintimmature neutrophils contribute to eradication ofS. pneumoniae. J. Exp. Med. *214*, 1333–
640 1350.

641 Dibo, M., Battocchio, E.C., dos Santos Souza, L.M., da Silva, M.D.V., Banin-Hirata, B.K., Sapla,
642 M.M.M., Marinello, P., Rocha, S.P.D., and Faccin-Galhardi, L.C. (2019). Antibody Therapy for the
643 Control of Viral Diseases: An Update. CPB *20*, 1108–1121.

644 DiLillo, D.J., and Ravetch, J.V. (2015). Differential Fc-Receptor Engagement Drives an Anti-tumor
645 Vaccinal Effect. Cell *161*, 1035–1045.

646 Earnest, J.T., Basore, K., Roy, V., Bailey, A.L., Wang, D., Alter, G., Fremont, D.H., and Diamond,
647 M.S. (2019). Neutralizing antibodies against Mayaro virus require Fc effector functions for protective
648 activity. Journal of Experimental Medicine *216*, 2282–2301.

649 Fan, Y., Wang, L., and Dou, X. (2018). Serum Monocyte Chemoattractant Protein-1 Predicts Liver
650 Inflammation of Patients with Chronic Hepatitis B. Clin. Lab. *64*.

651 Fox, J.M., Roy, V., Gunn, B.M., Huang, L., Edeling, M.A., Mack, M., Fremont, D.H., Doranz, B.J.,
652 Johnson, S., Alter, G., et al. (2019). Optimal therapeutic activity of monoclonal antibodies against
653 chikungunya virus requires Fc-FcγR interaction on monocytes. Sci. Immunol. *4*, eaav5062.

654 Gaylo-Moynihan, A., Prizant, H., Popović, M., Fernandes, N.R.J., Anderson, C.S., Chiou, K.K., Bell,
655 H., Schrock, D.C., Schumacher, J., Capece, T., et al. (2019). Programming of Distinct Chemokine-
656 Dependent and -Independent Search Strategies for Th1 and Th2 Cells Optimizes Function at Inflamed
657 Sites. Immunity *51*, 298-309.e6.

658 Gros, L., Dreja, H., Fiser, A.L., Plays, M., Pelegrin, M., and Piechaczyk, M. (2005). Induction of long-
659 term protective antiviral endogenous immune response by short neutralizing monoclonal antibody
660 treatment. J. Virol. *79*, 6272–6280.

661 Gros, L., Pelegrin, M., Michaud, H.-A., Bianco, S., Hernandez, J., Jacquet, C., and Piechaczyk, M.
662 (2008). Endogenous cytotoxic T-cell response contributes to the long-term antiretroviral protection
663 induced by a short period of antibody-based immunotherapy of neonatally infected mice. J. Virol. *82*,
664 1339–1349.

665 Gunn, B.M., Yu, W.-H., Karim, M.M., Brannan, J.M., Herbert, A.S., Wec, A.Z., Halfmann, P.J.,
666 Fusco, M.L., Schendel, S.L., Gangavarapu, K., et al. (2018). A Role for Fc Function in Therapeutic
667 Monoclonal Antibody-Mediated Protection against Ebola Virus. Cell Host & Microbe *24*, 221-233.e5.

668 Haider, C., Hnat, J., Wagner, R., Huber, H., Timelthaler, G., Grubinger, M., Coulouarn, C., Schreiner,
669 W., Schlangen, K., Sieghart, W., et al. (2019). Transforming Growth Factor-β and Axl Induce CXCL5
670 and Neutrophil Recruitment in Hepatocellular Carcinoma: HEPATOBILIARY MALIGNANCIES.
671 Hepatology *69*, 222–236.

672 Hildenbrand, B., Lorenzen, D., Sauer, B., Hertkorn, C., Freudenberg, M.A., Peters, J.H., Nesselhut, T.,
673 Unger, C., and Azemar, M. (2008). IFN-y enhances T(H)1 polarisation of monocyte-derived dendritic
674 cells matured with clinical-grade cytokines using serum-free conditions. Anticancer Res. *28*, 1467–
675 1476.

676 Hokeness, K.L., Kuziel, W.A., Biron, C.A., and Salazar-Mather, T.P. (2005). Monocyte
677 Chemoattractant Protein-1 and CCR2 Interactions Are Required for IFN- / -Induced Inflammatory
678 Responses and Antiviral Defense in Liver. The Journal of Immunology *174*, 1549–1556.

679 Hooft van Huijsduijnen, R., Kojima, S., Carter, D., Okabe, H., Sato, A., Akahata, W., Wells, T.N.C.,
680 and Katsuno, K. (2020). Reassessing therapeutic antibodies for neglected and tropical diseases. PLoS
681 Negl Trop Dis *14*, e0007860.

682 Jin, P., Zhao, Y., Liu, H., Chen, J., Ren, J., Jin, J., Bedognetti, D., Liu, S., Wang, E., Marincola, F., et
683 al. (2016). Interferon-γ and Tumor Necrosis Factor-α Polarize Bone Marrow Stromal Cells Uniformly
684 to a Th1 Phenotype. Sci Rep *6*, 26345.

685 Kelly-Scumpia, K.M., Scumpia, P.O., Delano, M.J., Weinstein, J.S., Cuenca, A.G., Wynn, J.L., and
686 Moldawer, L.L. (2010). Type I interferon signaling in hematopoietic cells is required for survival in
687 mouse polymicrobial sepsis by regulating CXCL10. The Journal of Experimental Medicine *207*, 319–
688 326.

689 Kim, Y.-G., Kamada, N., Shaw, M.H., Warner, N., Chen, G.Y., Franchi, L., and Núñez, G. (2011).
690 The Nod2 Sensor Promotes Intestinal Pathogen Eradication via the Chemokine CCL2-Dependent
691 Recruitment of Inflammatory Monocytes. Immunity *34*, 769–780.

692 Lambour, J., Naranjo-Gomez, M., Piechaczyk, M., and Pelegrin, M. (2016). Converting monoclonal
693 antibody-based immunotherapies from passive to active: bringing immune complexes into play.
694 Emerg Microbes Infect *5*, e92.

695 Lehmann, B., Biburger, M., Brückner, C., Ipsen-Escobedo, A., Gordan, S., Lehmann, C., Voehringer,
696 D., Winkler, T., Schaft, N., Dudziak, D., et al. (2017). Tumor location determines tissue-specific
697 recruitment of tumor-associated macrophages and antibody-dependent immunotherapy response. Sci.
698 Immunol. *2*, eaah6413.

699 Leonard, E.J., and Yoshimura, T. (1990). Human monocyte chemoattractant protein-1 (MCP-1).
700 Immunol. Today *11*, 97–101.

701 Liu, Q., Fan, C., Li, Q., Zhou, S., Huang, W., Wang, L., Sun, C., Wang, M., Wu, X., Ma, J., et al.
702 (2017). Antibody-dependent-cellular-cytotoxicity-inducing antibodies significantly affect the post-
703 exposure treatment of Ebola virus infection. Sci Rep *7*, 45552.

704 Lok, L.S.C., Dennison, T.W., Mahbubani, K.M., Saeb-Parsy, K., Chilvers, E.R., and Clatworthy, M.R.
705 (2019). Phenotypically distinct neutrophils patrol uninfected human and mouse lymph nodes. Proc
706 Natl Acad Sci USA *116*, 19083–19089.

707 Lu, L.L., Suscovich, T.J., Fortune, S.M., and Alter, G. (2018). Beyond binding: antibody effector
708 functions in infectious diseases. Nat. Rev. Immunol. *18*, 46–61.

709 Mantovani, A., Cassatella, M.A., Costantini, C., and Jaillon, S. (2011). Neutrophils in the activation
710 and regulation of innate and adaptive immunity. Nat. Rev. Immunol. *11*, 519–531.

711 McAtee, F.J., and Portis, J.L. (1985). Monoclonal antibodies specific for wild mouse neurotropic
712 retrovirus: detection of comparable levels of virus replication in mouse strains susceptible and
713 resistant to paralytic disease. J. Virol. *56*, 1018–1022.

714 Meinderts, S.M., Baker, G., van Wijk, S., Beuger, B.M., Geissler, J., Jansen, M.H., Saris, A., ten
715 Brinke, A., Kuijpers, T.W., van den Berg, T.K., et al. (2019). Neutrophils acquire antigen-presenting
716 cell features after phagocytosis of IgG-opsonized erythrocytes. Blood Advances *3*, 1761–1773.

717 Michaud, H.-A., Gomard, T., Gros, L., Thiolon, K., Nasser, R., Jacquet, C., Hernandez, J.,
718 Piechaczyk, M., and Pelegrin, M. (2010). A crucial role for infected-cell/antibody immune complexes
719 in the enhancement of endogenous antiviral immunity by short passive immunotherapy. PLoS Pathog.
720 *6*, e1000948.

721 Miller, A.L., Bowlin, T.L., and Lukacs, N.W. (2004). Respiratory Syncytial Virus–Induced
722 Chemokine Production: Linking Viral Replication to Chemokine Production In Vitro and In Vivo. J
723 INFECT DIS *189*, 1419–1430.

724 Morquin, D., Tuaillon, E., Makinson, A., Bendriss, S., Le Moing, V., and Reynes, J. (2017). Impact of
725 T cell activation, HIV replication and hepatitis C virus infection on neutrophil CD64 expression.
726 Cytometry B Clin Cytom *92*, 492–497.

727 Naranjo-Gomez, M., and Pelegrin, M. (2019). Vaccinal effect of HIV-1 antibody therapy: Current
728 Opinion in HIV and AIDS *14*, 325–333.

729 Naranjo-Gomez, M., Lambour, J., Piechaczyk, M., and Pelegrin, M. (2018). Neutrophils are essential
730 for induction of vaccine-like effects by antiviral monoclonal antibody immunotherapies. JCI Insight *3*.

731 Nasser, R., Pelegrin, M., Michaud, H.-A., Plays, M., Piechaczyk, M., and Gros, L. (2010). Long-
732 lasting protective antiviral immunity induced by passive immunotherapies requires both neutralizing
733 and effector functions of the administered monoclonal antibody. J. Virol. *84*, 10169–10181.

734 Ng, L.G., Ostuni, R., and Hidalgo, A. (2019). Heterogeneity of neutrophils. Nat Rev Immunol *19*,
735 255–265.

736 Niessl, J., Baxter, A.E., Mendoza, P., Jankovic, M., Cohen, Y.Z., Butler, A.L., Lu, C.-L., Dubé, M.,
737 Shimeliovich, I., Gruell, H., et al. (2020). Combination anti-HIV-1 antibody therapy is associated with
738 increased virus-specific T cell immunity. Nat Med *26*, 222–227.

739 Pelegrin, M., Naranjo-Gomez, M., and Piechaczyk, M. (2015). Antiviral Monoclonal Antibodies: Can
740 They Be More Than Simple Neutralizing Agents? Trends Microbiol. *23*, 653–665.

741 Portis, J.L., Czub, S., Garon, C.F., and McAtee, F.J. (1990). Neurodegenerative disease induced by the
742 wild mouse ecotropic retrovirus is markedly accelerated by long terminal repeat and gag-pol
743 sequences from nondefective Friend murine leukemia virus. J. Virol. *64*, 1648–1656.

744 Pricop, L., Redecha, P., Teillaud, J.L., Frey, J., Fridman, W.H., Sautès-Fridman, C., and Salmon, J.E.
745 (2001). Differential modulation of stimulatory and inhibitory Fc gamma receptors on human
746 monocytes by Th1 and Th2 cytokines. J. Immunol. *166*, 531–537.

747 Pruenster, M., Mudde, L., Bombosi, P., Dimitrova, S., Zsak, M., Middleton, J., Richmond, A.,
748 Graham, G.J., Segerer, S., Nibbs, R.J.B., et al. (2009). The Duffy antigen receptor for chemokines
749 transports chemokines and supports their promigratory activity. Nat Immunol *10*, 101–108.

750 Ritzman, A.M., Hughes-Hanks, J.M., Blaho, V.A., Wax, L.E., Mitchell, W.J., and Brown, C.R.
751 (2010). The Chemokine Receptor CXCR2 Ligand KC (CXCL1) Mediates Neutrophil Recruitment and
752 Is Critical for Development of Experimental Lyme Arthritis and Carditis. Infection and Immunity *78*,
753 4593–4600.

754 Robben, P.M., LaRegina, M., Kuziel, W.A., and Sibley, L.D. (2005). Recruitment of Gr-1+
755 monocytes is essential for control of acute toxoplasmosis. Journal of Experimental Medicine *201*,
756 1761–1769.

757 Rovai, L.E., Herschman, H.R., and Smith, J.B. (1998). The murine neutrophil-chemoattractant
758 chemokines LIX, KC, and MIP-2 have distinct induction kinetics, tissue distributions, and tissue-
759 specific sensitivities to glucocorticoid regulation in endotoxemia. J Leukoc Biol *64*, 494–502.

760 Rubio, N., and Sanz-Rodriguez, F. (2007). Induction of the CXCL1 (KC) chemokine in mouse
761 astrocytes by infection with the murine encephalomyelitis virus of Theiler. Virology *358*, 98–108.

762 Salazar, G., Zhang, N., Fu, T.-M., and An, Z. (2017). Antibody therapies for the prevention and
763 treatment of viral infections. NPJ Vaccines *2*, 19.

764 Scapini, P., Marini, O., Tecchio, C., and Cassatella, M.A. (2016). Human neutrophils in the saga of
765 cellular heterogeneity: insights and open questions. Immunol. Rev. *273*, 48–60.

766 Schoofs, T., Klein, F., Braunschweig, M., Kreider, E.F., Feldmann, A., Nogueira, L., Oliveira, T.,
767 Lorenzi, J.C.C., Parrish, E.H., Learn, G.H., et al. (2016). HIV-1 therapy with monoclonal antibody
768 3BNC117 elicits host immune responses against HIV-1. Science *352*, 997–1001.

769 Seo, S.-U., Kwon, H.-J., Ko, H.-J., Byun, Y.-H., Seong, B.L., Uematsu, S., Akira, S., and Kweon, M.-
770 N. (2011). Type I interferon signaling regulates Ly6C(hi) monocytes and neutrophils during acute
771 viral pneumonia in mice. PLoS Pathog. *7*, e1001304.

772 Silvestre-Roig, C., Hidalgo, A., and Soehnlein, O. (2016). Neutrophil heterogeneity: implications for
773 homeostasis and pathogenesis. Blood *127*, 2173–2181.

774 Silvestre-Roig, C., Fridlender, Z.G., Glogauer, M., and Scapini, P. (2019). Neutrophil Diversity in
775 Health and Disease. Trends in Immunology *40*, 565–583.

776 Tamassia, N., Bianchetto-Aguilera, F., Arruda-Silva, F., Gardiman, E., Gasperini, S., Calzetti, F., and
777 Cassatella, M.A. (2018). Cytokine production by human neutrophils: revisiting the "dark side of the
778 moon." Eur. J. Clin. Invest. e12952.

779 Tannenbaum, C.S., Tubbs, R., Armstrong, D., Finke, J.H., Bukowski, R.M., and Hamilton, T.A.
780 (1998). The CXC chemokines IP-10 and Mig are necessary for IL-12-mediated regression of the
781 mouse RENCA tumor. J. Immunol. *161*, 927–932.

782 Tecchio, C., and Cassatella, M.A. (2016a). Neutrophil-derived chemokines on the road to immunity.
783 Semin. Immunol. *28*, 119–128.

784 Tecchio, C., and Cassatella, M.A. (2016b). Neutrophil-derived chemokines on the road to immunity.
785 Seminars in Immunology *28*, 119–128.

786 Tokunaga, R., Zhang, W., Naseem, M., Puccini, A., Berger, M.D., Soni, S., McSkane, M., Baba, H.,
787 and Lenz, H.-J. (2018). CXCL9, CXCL10, CXCL11/CXCR3 axis for immune activation – A target
788 for novel cancer therapy. Cancer Treatment Reviews *63*, 40–47.

789 Tsuda, Y., Takahashi, H., Kobayashi, M., Hanafusa, T., Herndon, D.N., and Suzuki, F. (2004). Three
790 Different Neutrophil Subsets Exhibited in Mice with Different Susceptibilities to Infection by
791 Methicillin-Resistant Staphylococcus aureus. Immunity *21*, 215–226.

792 Uciechowski, P., and Dempke, W.C.M. (2020). Interleukin-6: A Masterplayer in the Cytokine
793 Network. Oncology *98*, 131–137.

794 Vono, M., Lin, A., Norrby-Teglund, A., Koup, R.A., Liang, F., and Loré, K. (2017). Neutrophils
795 acquire the capacity for antigen presentation to memory CD4+ T cells in vitro and ex vivo. Blood *129*,
796 1991–2001.

797 Wang, Q., and Zhang, L. (2020). Broadly neutralizing antibodies and vaccine design against HIV-1
798 infection. Front. Med. *14*, 30–42.

799 Wang, Y., and Jönsson, F. (2019). Expression, Role, and Regulation of Neutrophil Fcγ Receptors.
800 Front. Immunol. *10*, 1958.

801 Wang, J.P., Kurt-Jones, E.A., Shin, O.S., Manchak, M.D., Levin, M.J., and Finberg, R.W. (2005).
802 Varicella-Zoster Virus Activates Inflammatory Cytokines in Human Monocytes and Macrophages via
803 Toll-Like Receptor 2. Journal of Virology *79*, 12658–12666.

804 Wang, X.-Y., Wang, B., and Wen, Y.-M. (2019). From therapeutic antibodies to immune complex
805 vaccines. Npj Vaccines *4*, 2.

806 Wareing, M.D., Lyon, A.B., Lu, B., Gerard, C., and Sarawar, S.R. (2004). Chemokine expression
807 during the development and resolution of a pulmonary leukocyte response to influenza A virus
808 infection in mice. Journal of Leukocyte Biology *76*, 886–895.

809 Wen, Y.-M., Mu, L., and Shi, Y. (2016). Immunoregulatory functions of immune complexes in
810 vaccine and therapy. EMBO Mol Med *8*, 1120–1133.

811 Yamamoto, T., Iwamoto, N., Yamamoto, H., Tsukamoto, T., Kuwano, T., Takeda, A., Kawada, M.,
812 Tsunetsugu-Yokota, Y., and Matano, T. (2009). Polyfunctional CD4+ T-cell induction in neutralizing
813 antibody-triggered control of simian immunodeficiency virus infection. J. Virol. *83*, 5514–5524.

814 Yoshida, T., Kobayashi, M., Li, X.-D., Pollard, R.B., and Suzuki, F. (2009). Inhibitory effect of
815 glycyrrhizin on the neutrophil-dependent increase of R5 HIV replication in cultures of macrophages.
816 Immunol Cell Biol *87*, 554–558.

817

818

819 **FIGURE LEGENDS**

820

821 ***Figure 1:*** **Phenotypic and functional activation of neutrophils stimulated with FrCas^E virions**
822 **and ICs. A.** *Experimental scheme*. **B**. *Phenotypic activation of neutrophils stimulated by FrCas^E*
823 *virions or viral ICs made with the 667 mAb*. V, free virions; IC, viral ICs; M, culture medium. Free
824 667 mAb was used as control. Activation was assessed by monitoring CD11b expression and
825 frequency of CD11b^{hi} CD62L^{lo} neutrophils. The data represent 12 independent experiments. **C**.
826 *Functional activation of neutrophils stimulated by FrCas^E virions (V) or viral ICs made with the 667*
827 *mAb (IC)*. Chemokines release was assessed in supernatants of neutrophils isolated from BM of naive
828 mice (>97-98% purity) and stimulated for 24 h by FrCas^E virions (red) or viral ICs (blue) or left
829 unstimulated (grey). The data represent 5 independent experiments. Data are expressed as means +/-
830 SEM. Statistical significance was established using a parametric 1-way ANOVA test (*$p < 0.05$; **$p <$
831 0.01; ***$p < 0.001$).

832

833 ***Figure 2:*** **Phenotypic and functional activation of monocytes stimulated with FrCas^E virions and**
834 **ICs. A.** *Experimental scheme*. **B**. *Phenotypic activation of monocytes stimulated by FrCas^E virions or*
835 *viral ICs made with the 667 mAb*. Free 667 mAb was used as control. V, free virions; IC, viral ICs; M,
836 culture medium. Activation was assessed by monitoring CD86 expression. The data represent 7
837 independent experiments **C**. *Functional activation of monocytes stimulated by FrCas^E virions (V) or*
838 *viral ICs made with the 667 mAb (IC). C*hemokines release was assessed in supernatants of monocytes
839 isolated from BM of naive mice (>97-98% purity) and stimulated for 24 h by FrCas^E virions (red) or
840 viral ICs (blue) or left unstimulated (grey). The data represent 5 independent experiments. Data are
841 expressed as means +/- SEM. Statistical significance was established using a parametric 1-way
842 ANOVA test (*$p < 0.05$; **$p < 0.01$; ***$p < 0.001$).

843

844 ***Figure 3:*** **Cytokine priming potentialize the functional activation of neutrophils and monocytes**
845 **by ICs.** BM-derived neutrophils and monocytes were isolated from naive mice and activated as in
846 **Figures 1 and 2** in the presence, or in the absence, of *TNFα, IFN-I or IFNγ.* **(A, C).** *Phenotypic*
847 *activation of activated neutrophils (**A**) and monocytes (**C**) by TNFα, IFN-I or IFNγ.* Activation was
848 assessed by monitoring CD11b (**A**) and CD86 expression **(C)**. *Modulation of the functional activation*
849 *of neutrophils and monocytes by TNFα, IFN-I or IFNγ.* **(B, D).** Chemokines and cytokines release
850 were assessed in supernatants of activated neutrophils and monocytes. Histograms depict the increase
851 in cytokine/chemokine release upon priming of virus- and IC-activated neutrophils by *TNFα, IFN-I or*
852 *IFNγ* (calculated as the difference in the amount of chemokine/cytokine secretion by V- or IC-
853 stimulated neutrophils in the absence or in the presence of priming; **Supplemental figure 3**). Only
854 those chemokines/cytokines significantly enhanced by cytokine priming are depicted. The data

855 represent 6 independent experiments for **A**, 4 independent experiments for **B** and 3 independent
856 experiments for **C** and **D**. Data are expressed as means +/- SEM. Diamonds indicate significant
857 differences to all the other stimulation conditions (black diamond) or to corresponding medium
858 without virus or IC stimuli (grey diamond) as determined by Kruskal-Wallis tests ($p < 0.05$).
859
860 ***Figure 4:*** **FcγRIV is upregulated by IFN priming on both neutrophils and monocytes cell**
861 **surface.** Neutrophils and monocytes were isolated from naive mice and stimulated as in **Figure 3**.
862 FcγRIV expression was evaluated on neutrophils **(A, B)** and monocytes **(C, D)** in absence (**A, C**) or in
863 the presence of TNFα, IFN-I or IFNγ (**B, D**). The data represent 5 independent experiments for
864 neutrophils (**A, B**) and 3 independent experiments for monocytes (**C, D**). Data are expressed as means
865 +/- SEM. Diamonds indicate significant differences to the corresponding stimuli in the absence of
866 cytokine priming (open diamond) or to corresponding medium without virus or IC stimuli (grey
867 diamond) as determined by Kruskal-Wallis tests ($p < 0.05$).
868
869 ***Figure 5:*** **FcγRIV is upregulated *in vivo* on two different splenic neutrophils subpopulations and**
870 **on inflammatory monocytes.** Splenocytes from naive (grey), infected/non-treated (I/NT; red) and
871 infected/treated (I/T;blue) mice were analyzed on days 8 (D8) and 14 (D14) p.i. for (i) neutrophils and
872 monocytes recruitment and (ii) for FcγRIV expression. (**A**) Gating strategy used to define neutrophils
873 and monocytes populations. (**B**) Frequencies of $CD11b^{+}Ly6G^{hi}$ and $CD11b^{+}Ly6G^{int}$ neutrophils
874 subpopulations as well as $Ly6C^{hi}$ monocytes in the $CD45.2^{+}$ leukocytic population. The data represent
875 5 independent experiments at D8 p.i. and 6 independent experiments at D14 p.i with at least 6-9 mice
876 per group (I/NT and I/T) and 3-5 mice per group (naive mice). (**C-D**) FcγRIV expression on
877 $CD11b^{+}Ly6G^{hi}$ and $CD11b^{+}Ly6G^{int}$ neutrophils subpopulations and $Ly6C^{hi}$ monocytes. The data
878 represent 5 independent experiments at D8 p.i. and 6 independent experiments at D14 p.i with at least
879 6-9 mice per group (I/NT and I/T) and 3-5 mice per group (naive mice). (**E**) Cell surface markers
880 expression of $CD11b^{+}Ly6G^{hi}$ and $CD11b^{+}Ly6G^{int}$ neutrophils and $Ly6C^{hi}$ monocytes isolated from 15-
881 days old naive mice, with 3-5 mice per group. Data are expressed as means +/- SEM. Statistical
882 significance was established using a parametric 1-way ANOVA test (*$p < 0.05$; **$p < 0.01$; ***$p <$
883 0.001).
884
885 ***Figure 6:*** **Cell surface activation markers expression on two different splenic neutrophils**
886 **subpopulations and on inflammatory monocytes.** Splenocytes from naive (grey), infected/non-
887 treated (I/NT; red) and infected/treated (I/T;blue) mice were analyzed on days 8 (**A**) and 14 p.i. (**B**) for
888 neutrophils and monocytes expression of CD11b, CD86 and MHC-II. Data represent 5 independent
889 experiments at D8 p.i. and 6 independent experiments at D14 p.i with at least 6-9 mice per group
890 (I/NT and I/T) and 3-5 mice per group (naive mice). Data are expressed as means +/- SEM. Statistical

891 significance was established using a parametric 1-way ANOVA test (*p < 0.05; **p < 0.01; ***p <
892 0.001).
893
894 ***Figure 7:*** **Cytokine and chemokine secretion profile of two different splenic neutrophils**
895 **subpopulations and on inflammatory monocytes.** Splenic neutrophils subpopulations and
896 inflammatory monocytes from naive, infected/non-treated (I) and infected/treated mice (IT) were
897 isolated at days 8 p.i. and 14 p.i. for assaying their chemokine and cytokine secretion profile in
898 supernatants of sorted cells cultured at a density of $4x10^6$ cells/ml ($1x10^6$ cells/well) for 24 h. Data
899 represent 3 independent experiments on D8 p.i. and 4 independent experiments on D14 p.i. with at
900 least 6-8 mice per group. (**A**) Total quantity of chemokines and cytokines secreted by neutrophils
901 subpopulations and inflammatory monocytes from infected/non-treated and infected/treated mice. (**B**)
902 Chemokine and cytokine secretion of neutrophils subpopulations and inflammatory monocytes
903 isolated from naive, infected/non-treated (I) and infected/treated mice (IT). The color code shows fold-
904 increase compared to secretion detected in cells isolated from naive mice (the raw chemokine and
905 cytokine release values are given in brackets, expressed in pg/ml). (**C**) Chemokine and cytokine
906 secretion of neutrophils subpopulations and inflammatory monocytes isolated from infected/non-
907 treated (I) and infected/treated mice (IT) expressed as percentage of chemokine and cytokine showing
908 a fold-increase ≥1.4 as compared to cells isolated from naive mice.
909
910 **SUPPLEMENTAL FIGURE LEGENDS**
911 ***Supplemental Figure 1.*** **Functional activation of neutrophils stimulated with viral determinants**
912 **or LPS.** BM-derived neutrophils were isolated from naive mice and stimulated for 24h *in vitro* with
913 viral determinants (virus or ICs) or LPS (1μg/ml). **A**. *Cytokine secretion profile of neutrophils*
914 *stimulated by virus (red) o viral ICs (blue) or unstimulated (grey)*. Cytokine release was assessed in
915 supernatants of neutrophils isolated from BM of naive mice (>97-98% purity). Data represent 5
916 independent experiments and are expressed as means +/- SEM. Statistical significance was established
917 using a parametric 1-way ANOVA test (*p < 0.05; **p < 0.01; ***p < 0.001). **B-D**. *Functional*
918 *activation of neutrophils stimulated by LPS*. Activation was assessed by monitoring CD11b expression
919 and frequency of $CD11b^{hi}$ $CD62L^{lo}$ neutrophils (**B**) as well as the cytokines (**C**) and chemokines (**D**)
920 released in supernatants of neutrophils stimulated for 24 h by LPS (green) or left unstimulated (grey).
921 Data represent 12 independent experiments and are expressed as means +/- SEM. Statistical
922 significance was established using a paired Student's t test (*p < 0.05; **p < 0.01; ***p < 0.001).
923
924 ***Supplemental Figure 2:*** **Functional activation of monocytes stimulated with viral determinants**
925 **or LPS.** BM-derived monocytes were isolated from naive mice and stimulated for 24h *in vitro* with
926 viral determinants (virus or IC) or LPS (1μg/ml). **A**. *Cytokine secretion profile of monocytes*

927 *stimulated by virus (red) o viral ICs (blue) or unstimulated (grey)*. Cytokine release was assessed in
928 supernatants of monocytes isolated from BM of naive mice (>97-98% purity) and stimulated for 24 h.
929 The data represent 6 independent experiments and are expressed as means +/- SEM. Statistical
930 significance was established using a parametric 1-way ANOVA test (*$p < 0.05$; **$p < 0.01$; ***$p <$
931 0.001). **B-D**. *Functional activation of monocytes stimulated by LPS*. Activation was assessed by
932 monitoring the CD86 expression level (**B**) as well as the cytokines (**C**) and chemokines (**D**) release
933 monitored in supernatants of monocytes stimulated for 24 h by LPS (green) or left unstimulated
934 (grey). Data represent 5 independent experiments and are expressed as means +/- SEM. Statistical
935 significance was established using a paired Student's t test (*$p < 0.05$; **$p < 0.01$; ***$p < 0.001$).
936
937 ***Supplemental Figure 3.*** **Cytokine priming enhance chemokine/cytokine release by IC-activated**
938 **neutrophils and monocytes**. BM-derived neutrophils and monocytes were isolated from naive mice
939 and activated as in **Figures 1 and 2** in the presence, or in the absence, of TNFα, IFN-I or IFNγ.
940 Chemokines and cytokines release were assessed in supernatants of activated neutrophils (**A**) and
941 monocytes (**B**). Only those chemokines/cytokines significantly enhanced by cytokine priming are
942 depicted. The data represent 4 independent experiments for **A** and 3 independent experiments for **B**.
943 Diamonds indicate significant differences to all the other stimulation conditions (black diamond), or to
944 corresponding medium without virus or ICs stimuli (grey diamond), or to the corresponding stimuli in
945 the absence of cytokine priming (open diamond), as determined by Kruskal Wallis test ($p < 0.05$).
946
947 ***Supplemental Figure 4:*** **FcγRI and FcγRII-III *in vitro* expression on neutrophils and monocytes**
948 **stimulated with viral determinants, in the presence and the absence of TNFα, IFN-I or IFNγ.**
949 FcγRII-III and FcγRI expression was monitored on neutrophils **(A)** and monocytes **(B).** No FcγRI
950 expression was detected on neutrophils. The data represent 6 independent experiments for **A** et 4
951 independent experiments for **B**. Data are expressed as means +/- SEM. Diamonds indicate significant
952 differences from the corresponding stimuli in the absence of cytokine priming (open diamond), or
953 from all the other stimulation conditions (black diamond) or from corresponding medium without
954 virus or ICs stimuli (grey diamond) as determined by Kruskal Wallis test ($p < 0.05$).
955
956 ***Supplemental Figure 5:*** **FcγRI and FcγRII-III *in vivo* expression on two different splenic**
957 **neutrophils subpopulations and on inflammatory monocytes.** Splenocytes from naïve (grey,
958 infected/non-treated (I/NT;red) and infected/treated (I/T; blue) mice were analyzed on days 8 (**A**) and
959 14 p.i. (**B**) for FcγRII-III and FcγRI expression on $CD11b^{+}Ly6G^{hi}$ and $CD11b^{+}Ly6G^{int}$ neutrophils
960 subpopulations and $Ly6C^{hi}$ monocytes. Data represent 5 independent experiments at D8 p.i. and 6
961 independent experiments at D14 p.i with at least 6-9 mice per group (I/NT and I/T) and 3-5 mice per

962 group (naive mice). Data are expressed as means +/- SEM. Statistical significance was established
963 using a parametric 1-way ANOVA test (*$p < 0.05$; **$p < 0.01$; ***$p < 0.001$).
964

A

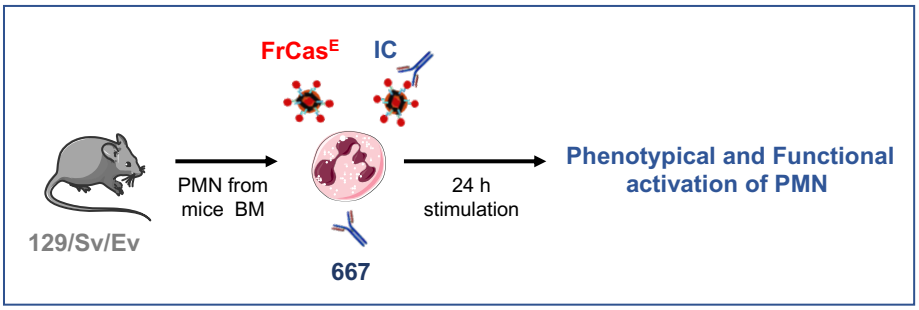
FrCas^E
IC
129/Sv/Ev
PMN from mice BM
667
24 h stimulation
Phenotypical and Functional activation of PMN

B

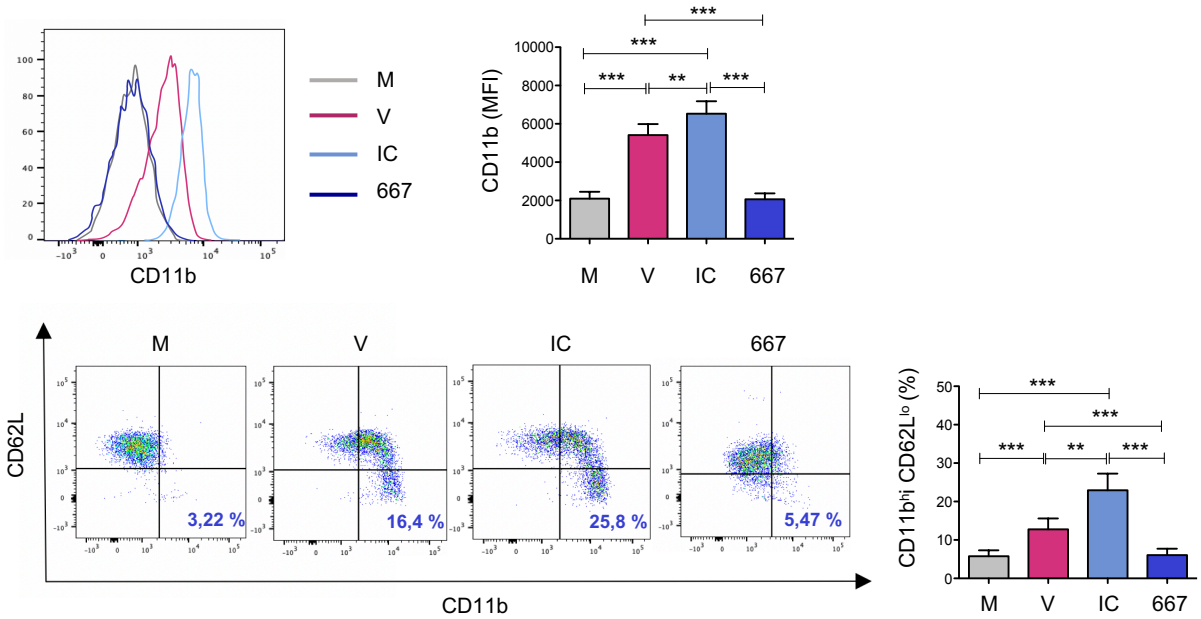
CD11b
M
V
IC
667
CD11b (MFI)
M V IC 667
CD62L
CD11b
3,22 %
16,4 %
25,8 %
5,47 %
CD11b^{hi} CD62L^{lo} (%)

C

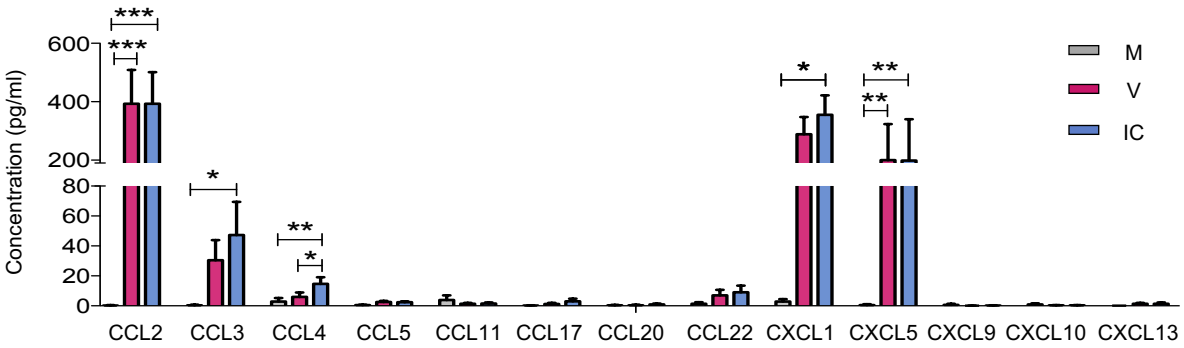
Concentration (pg/ml)
M
V
IC
CCL2 CCL3 CCL4 CCL5 CCL11 CCL17 CCL20 CCL22 CXCL1 CXCL5 CXCL9 CXCL10 CXCL13

Figure 1

A

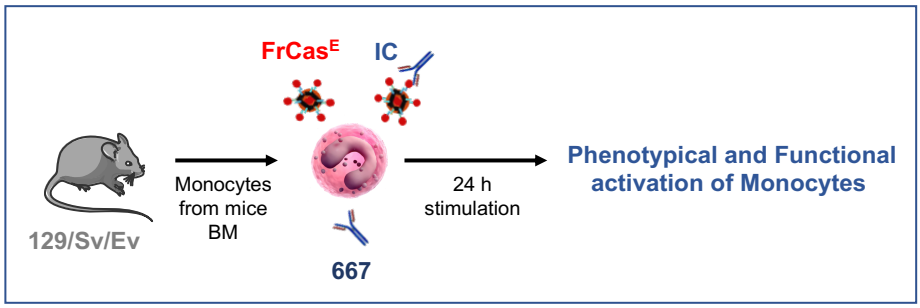
FrCas^E
IC
129/Sv/Ev
Monocytes from mice BM
667
24 h stimulation
Phenotypical and Functional activation of Monocytes

B

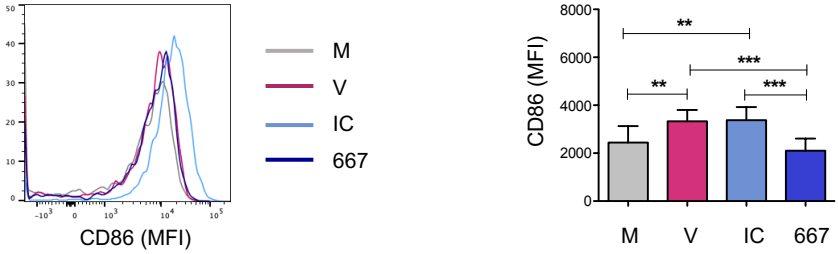
CD86 (MFI)
M
V
IC
667
CD86 (MFI)
8000
6000
4000
2000
0
**
***
**
***
M
V
IC
667

C

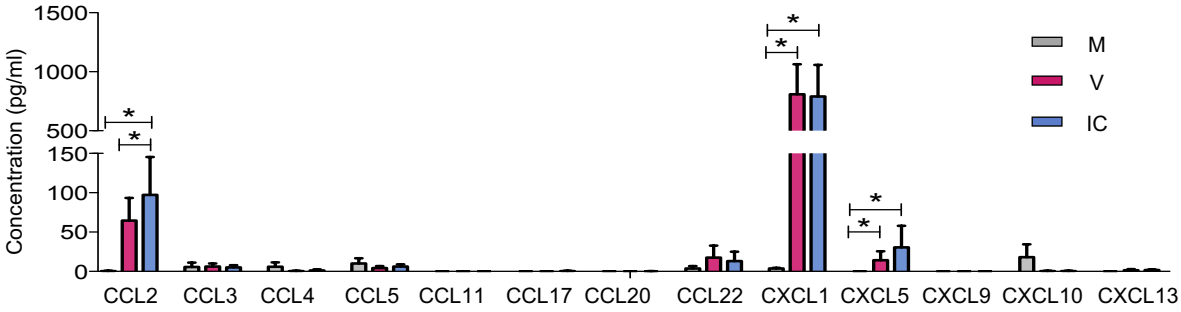
Concentration (pg/ml)
1500
1000
500
150
100
50
0
*
*
*
*
*
*
M
V
IC
CCL2
CCL3
CCL4
CCL5
CCL11
CCL17
CCL20
CCL22
CXCL1
CXCL5
CXCL9
CXCL10
CXCL13

Figure 2

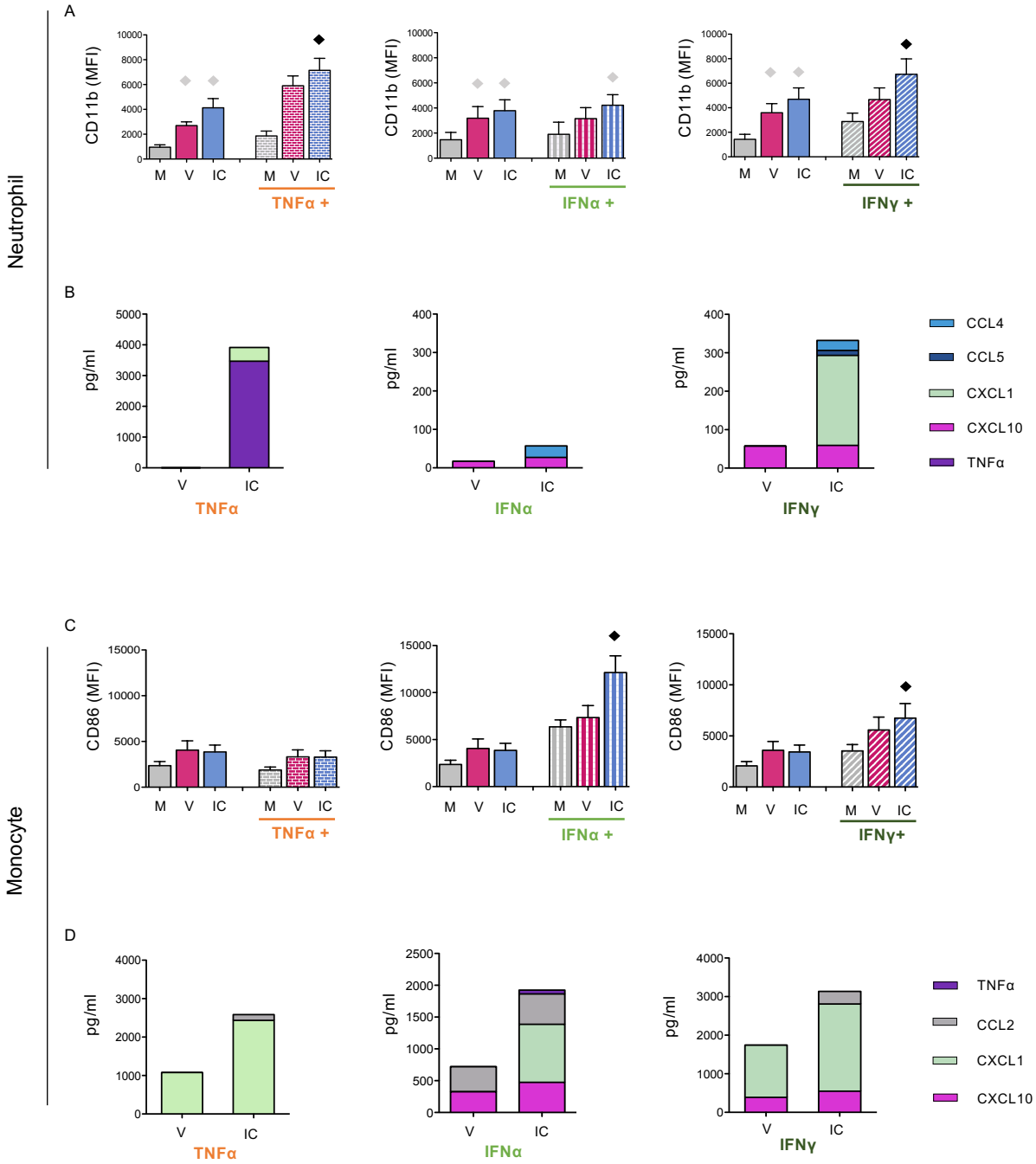
Neutrophil
A
CD11b (MFI)
M V IC M V IC
TNFα +
IFNα +
IFNγ +
B
pg/ml
V IC
TNFα
IFNα
IFNγ
CCL4
CCL5
CXCL1
CXCL10
TNFα
Monocyte
C
CD86 (MFI)
TNFα +
IFNα +
IFNγ+
D
CCL2

Figure 3

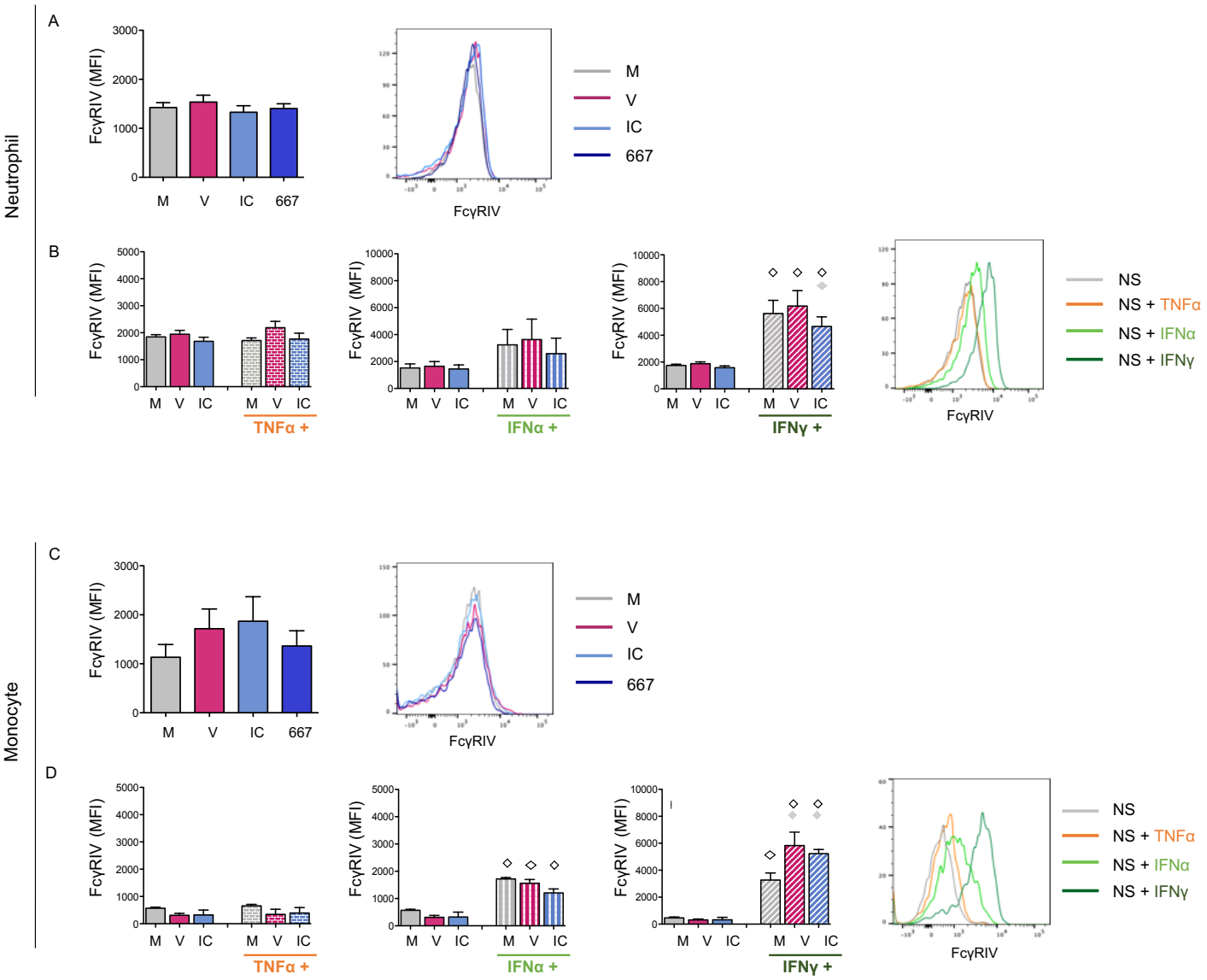
Neutrophil
A
FcγRIV (MFI)
M
V
IC
667
FcγRIV
B
TNFα +
IFNα +
IFNγ +
NS
NS + TNFα
NS + IFNα
NS + IFNγ
Monocyte
C
D

Figure 4

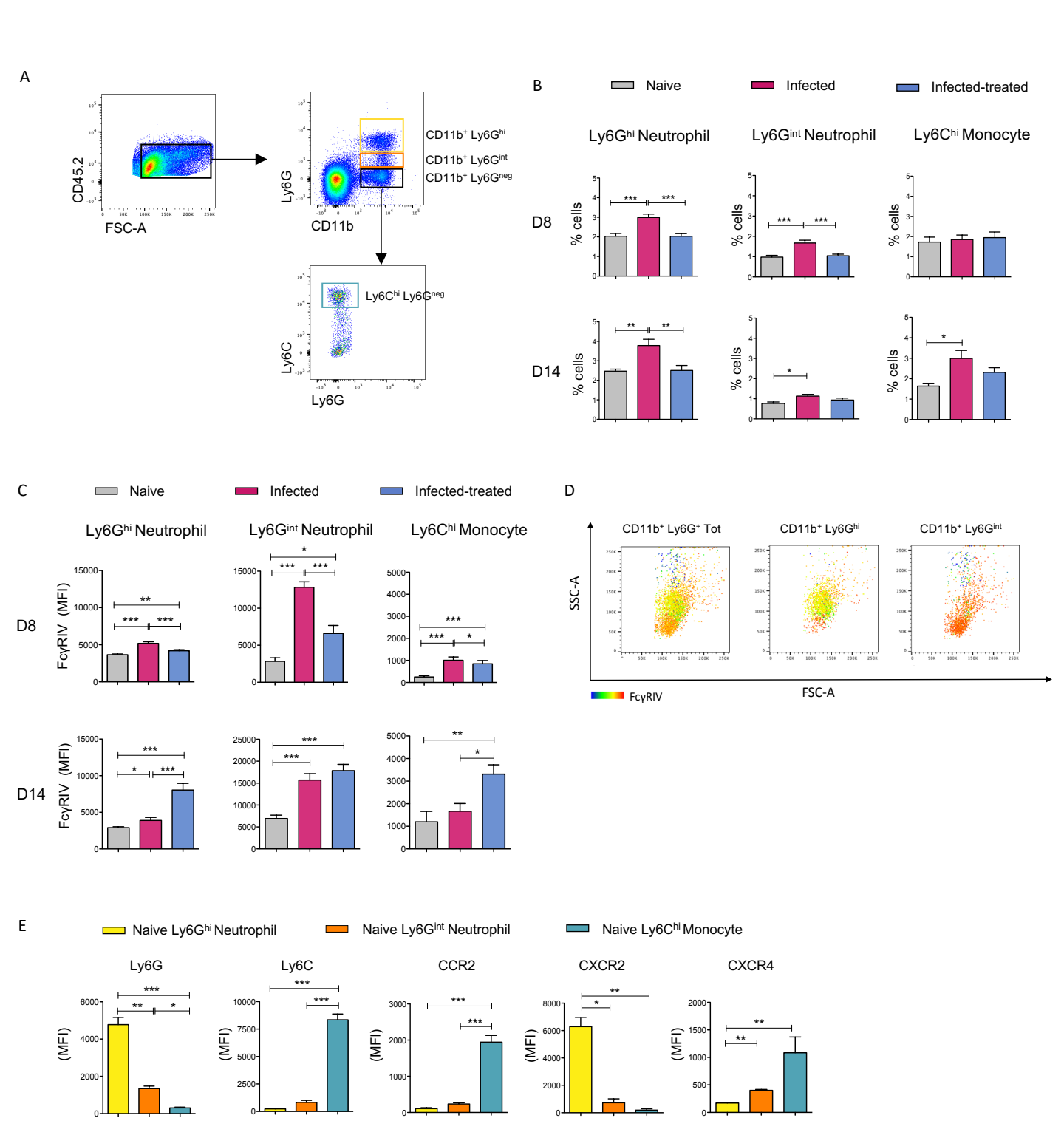
A
CD45.2
FSC-A
Ly6G
CD11b
CD11b+ Ly6Ghi
CD11b+ Ly6Gint
CD11b+ Ly6Gneg
Ly6C
Ly6G
Ly6Chi Ly6Gneg
B
Naive
Infected
Infected-treated
Ly6Ghi Neutrophil
Ly6Gint Neutrophil
Ly6Chi Monocyte
D8
D14
% cells
C
FcγRIV (MFI)
D
CD11b+ Ly6G+ Tot
CD11b+ Ly6Ghi
CD11b+ Ly6Gint
SSC-A
FSC-A
FcγRIV
E
Naive Ly6Ghi Neutrophil
Naive Ly6Gint Neutrophil
Naive Ly6Chi Monocyte
Ly6G
Ly6C
CCR2
CXCR2
CXCR4
(MFI)

Figure 5

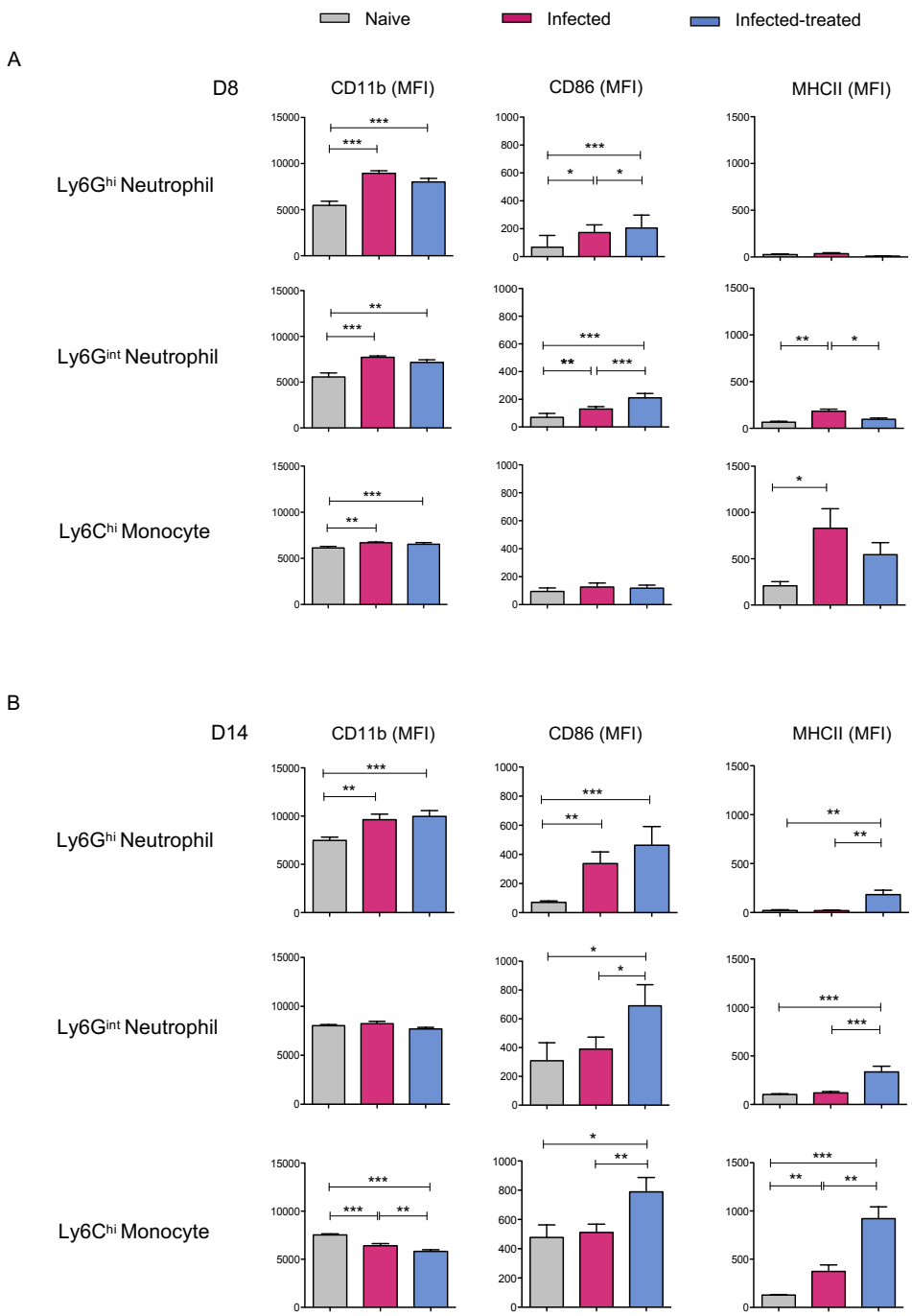
Naive
Infected
Infected-treated
A
D8
CD11b (MFI)
CD86 (MFI)
MHCII (MFI)
Ly6G^{hi} Neutrophil
Ly6G^{int} Neutrophil
Ly6C^{hi} Monocyte
B
D14
CD11b (MFI)
CD86 (MFI)
MHCII (MFI)
Ly6G^{hi} Neutrophil
Ly6G^{int} Neutrophil
Ly6C^{hi} Monocyte

Figure 6

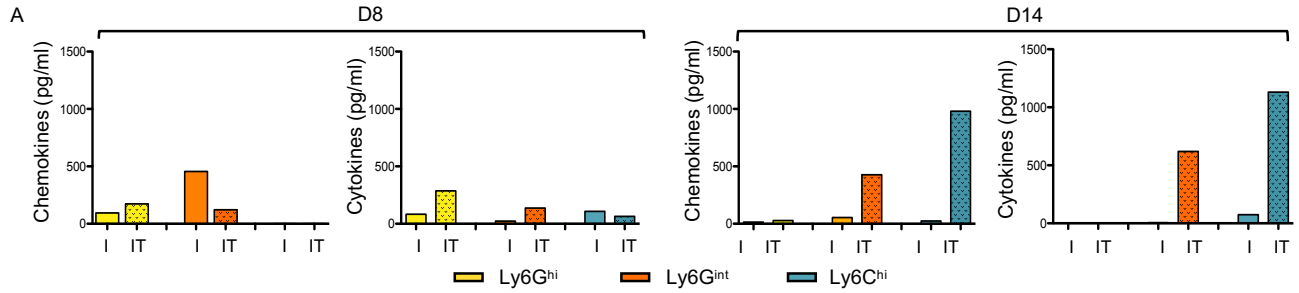

B

D8 — Chemokines

	Ly6Ghi Naive	Ly6Ghi I	Ly6Ghi IT	Ly6Gint Naive	Ly6Gint I	Ly6Gint IT	Ly6Chi Naive	Ly6Chi I	Ly6Chi IT
CCL2	1 (7)	1,4	1,4	1 (8,7)	1,7	1,2	1 (17)	0,8	0,8
CCL3				1 (1,6)	11,3	3,3	1 (21)	0,7	1,1
CCL4	1 (18)	2,1	2,7	1 (39)	1,6	1,6	1 (272)	0,3	0,4
CCL5	1 (8,4)	1,9	1,9	1 (3,8)	36,7	19,5	1(375)	0,4	0,3
CCL11	1(6,4)	2	1,7	1 (9,4)	1,8	1	1(18)	0,8	0,7
CCL17	1 (10)	2	2,2	1 (16)	2,7	1	1 (45)	0,7	0,7
CCL20	1 (4,5)	2,4	1,7	1 (5,6)	2	1,2	1 (12)	0,8	0,7
CCL22	1 (7,3)	1,7	1,8	1 (12)	2,3	0,9	1 (19)	0,9	0,9
CXCL1	1 (7,3)	0,8	3,2	1 (7,2)	4	1,5	1 (24)	0,4	1,4
CXCL5	1 (29)	1,3	2,7	1 (29)	7,1	3,6	1 (202)	0,5	0,8
CXCL9	1 (6,3)	1,5	1,4	1 (6,8)	1,8	1,1	1 (16)	0,7	0,6
CXCL10				1 (10)	1,4	0,2	1 (151)	0,9	1,1
CXC13	1 (6,1)	1,2	1,4	1 (7,4)	1,6	1,1	1(16,7)	0,6	0,6

D14 — Chemokines

	Ly6Ghi Naive	Ly6Ghi I	Ly6Ghi IT	Ly6Gint Naive	Ly6Gint I	Ly6Gint IT	Ly6Chi Naive	Ly6Chi I	Ly6Chi IT
CCL2									
CCL3				1 (1)	1,3	34,8	1 (3,7)	0,4	1,9
CCL4	1 (1)	7,1	26,6	1 (8,5)	0,8	4,3	1 (10)	1,4	2,8
CCL5	1 (2,5)	1,1	1,4	1 (52)	1,4	3,1	1(100)	1,1	8,5
CCL11									
CCL17									
CCL20									
CCL22				1 (3,1)	11,8	53,7	1 (4,8)	1,8	15,9
CXCL1							1 (2,5)	0,9	8,5
CXCL5									
CXCL9				1 (1)	1	21,4			
CXCL10				1 (8,3)	0,8	10,2	1 (8,2)	2,1	13,4
CXC13									

D8 — Cytokines

	Ly6Ghi Naive	Ly6Ghi I	Ly6Ghi IT	Ly6Gint Naive	Ly6Gint I	Ly6Gint IT	Ly6Chi Naive	Ly6Chi I	Ly6Chi IT
IL1α							1 (4,1)	2,3	0,9
IL1β	1 (8,7)	2,2	2,7	1 (8,6)	1,2	2	1 (9,4)	2,2	1,6
IL6	1 (8,7)	1,2	2,2	1 (26)	0,6	1,3	1 (66)	0,5	0,7
IL10	1 (1,2)	15	12,7	1 (13)	0,7	1,3	1 (16)	0,9	0,4
IL12p70	1 (3,3)	2,7	2,7	1 (7,9)	1,1	1,6	1 (11)	1,4	0,8
IL17A	1 (6,1)	1,9	2,7	1 (11)	0,7	1,5	1 (13)	1,6	0,8
IL23	1 (3,2)	2,4	2,8	1 (5,4)	1	2,2	1 (9,6)	1	1
IL27	1 (13)	2,2	3,1	1 (14)	1,5	1,9	1 (11)	3,7	1,5
IFNβ	1 (3,4)	4,8	8,3	1 (36)	0,7	1,5	1 (73)	0,7	1,1
IFNγ	1 (8)	1,2	0,8	1 (5,6)	1,6	1,5	1 (6,1)	2,1	1,3
TNFα	1 (6)	2,3	3,4	1 (36)	0,8	0,9	1(611)	0,5	0,2
GM-CSF	1 (7,2)	1,9	2,4	1 (9,3)	1,3	1,4	1 (16)	1,2	0,6

D14 — Cytokines

	Ly6Ghi Naive	Ly6Ghi I	Ly6Ghi IT	Ly6Gint Naive	Ly6Gint I	Ly6Gint IT	Ly6Chi Naive	Ly6Chi I	Ly6Chi IT
IL1α									
IL1β									
IL6				1 (3,2)	1,8	93,6	1 (1,9)	33,4	296,4
IL10									
IL12p70									
IL17A									
IL23									
IL27									
IFNβ									
IFNγ				1 (0,4)	2,2	534,4	1 (0,8)	1,6	616
TNFα				1 (11)	0,4	10,3	1 (42)	1,1	2,9
GM-CSF									

0 1 10 50 100 >500

C

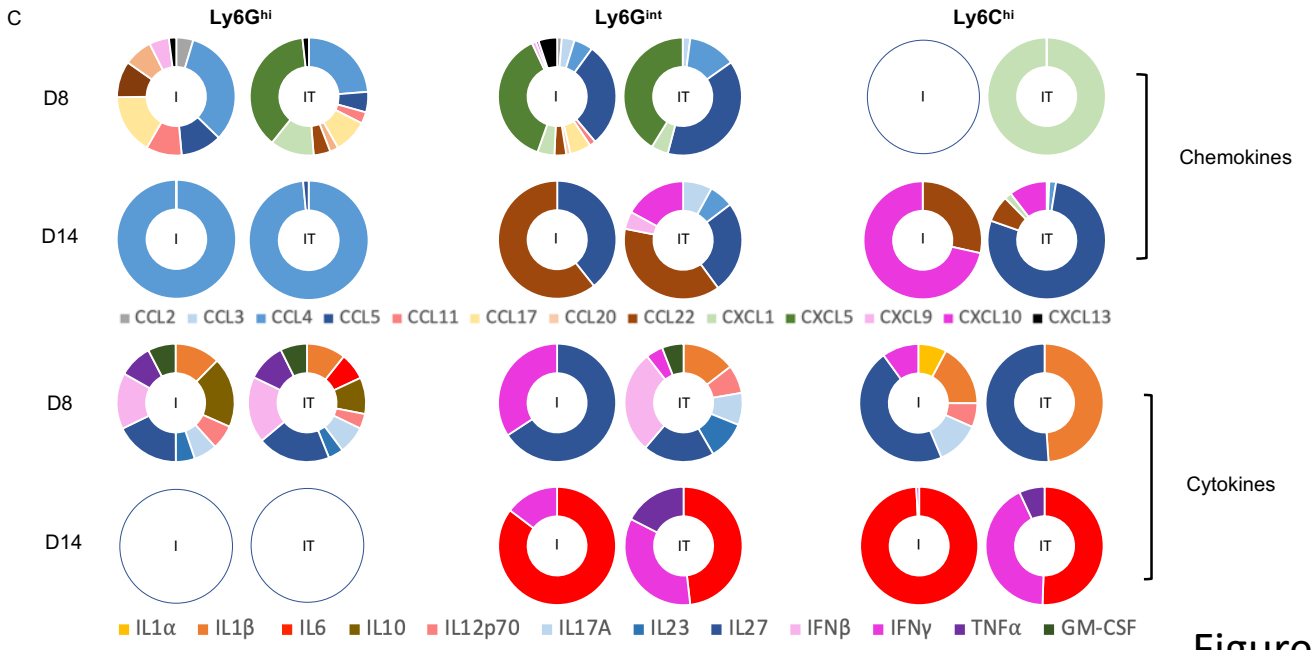

Figure 7